DE97007741
June 1997 • NREL/SR-540-23145 • ~~DE97050816~~ • UC Category: 1504

The Origin of Organic Pollutants from the Combustion of Alternative Fuels: Phase IV Report

Philip H. Taylor and Barry Dellinger
University of Dayton Research Institute
Other Contributors:
Sukh S. Sidhu
Wayne A. Rubey
Rich C. Striebich
Li Cheng

NREL Technical Monitors: Brent Bailey and Michelle Bergin

National Renewable Energy Laboratory
1617 Cole Boulevard
Golden, Colorado 80401-3393
A national laboratory of the
U.S. Department of Energy
Managed by the Midwest Research Institute
For the U.S. Department of Energy
Under Contract No. DE-AC36-83CH10093

Prepared under Subcontract Number XAU-3-12228-02
June 1997

NOTICE

Available to DOE and DOE contractors from:
Office of Scientific and Technical Information (OSTI)
P.O. Box 62
Oak Ridge, TN 37831
Prices available by calling (423) 576-8401

Available to the public from:
National Technical Information Service (NTIS)
U.S. Department of Commerce
5285 Port Royal Road
Springfield, VA 22161
(703) 487-4650

Executive Summary

As part of the US-DOE's on-going interest in the use of alternative automotive fuels, the University of Dayton Research Institute has been conducting research on pollutant emissions resulting from the combustion of candidate fuels. This research, under the direction and sponsorship of the NREL, has been concerned primarily with the combustion of compressed natural gas (CNG), liquefied petroleum gas (LPG), methanol, and ethanol.

In the first 24 months of this program, studies of the oxygen rich, stoichiometric, and fuel-rich thermal degradation of these fuels in the temperature range of 300 to 1100°C at atmospheric pressure and for reaction times of 1.0 and 2.0 s were completed. Trace organic products were identified and quantified for each fuel as a function of temperature. The results of these studies agreed well with the results of tail-pipe emission studies in that the types and quantity of emissions measured in both the laboratory and engine tests were shown to be very similar under certain operating conditions. However, some chemicals were observed in the laboratory studies that were not observed in the engine studies and vice versa. This result is important in that it has implications concerning the origin of these emissions.

As a consequence of these results, we developed a qualitative failure mode assessment of alternative fuel combustion and used it to identify additional experimental tasks to better understand the origin of organic emissions. These experimental tasks have focused on:

- advanced chromatographic measurements of thermally labile partial oxygenated products from the combustion of reformulated gasoline,
- the effects of NO_x on the oxidation of residual alcohol fuels,
- the effects of hydrocarbon fuel components on the oxidation of alcohol fuels,
- and the low temperature, surface catalyzed oxidation of residual alcohol fuels.

A major observation during the course of conducting the advanced chromatographic analysis of the RFG effluents was the intriguing nature of the various effluent products identified. A majority of these compounds, particularly the polar oxygenated species, have not been identified previously in engine tests on reformulated gasoline. The potential impact of such products with respect to environmental interactions and toxicological effects are currently areas of keen interest.

Experiments concerning the NO perturbed oxidation of methanol, M85, ethanol, and E85 indicated the presence of complex oxidation chemistry. At mild temperatures, NO addition resulted in enhanced fuel conversion. At elevated temperatures, an inhibitory effect was observed through increased yields of both partial oxidation and pyrolysis-type reaction products. Comparison of flow reactor product distributions with engine test results generally indicated improved comparisons when NO was added to the fuel.

Analysis of secondary components of alcohol fuels resulted in some unexpected observations. NMOG emissions from methanol, ethanol, M85 and E85 were observed to be more sensitive to exposure temperature than fuel/air equivalence ratio. Specific reactivities of M85 were observed to be substantially lower than for the other fuels. Several previously unidentified species were observed in these experiments which may impact atmospheric reactivity assessments of these fuels. A qualitative comparison of organic speciation for these fuels with recent engine tests produced remarkably similar results.

Laboratory-scale experiments of the conversion of neat methanol and ethanol over a Pd/Pt catalyst resulted in a number of partially oxidized reaction products that have not been reported in engine tests or laboratory gas-phase oxidation studies. These compounds have relatively low reactivities with OH radicals compared to the typically measured C_1-C_7 aldehyde byproducts. As a result, their impact on tropospheric smog formation may be fairly minimal. The health effect impacts of these compounds, on the other hand, may be a significant issue. Certain oxygen-containing compounds have been implicated as potential endocrine disrupter chemicals.

Table of Contents

List of Figures

List of Figures (continued)

List of Tables

Introduction

As part of the US-DOE's on-going interest in the use of alternative automotive fuels, the University of Dayton Research Institute has been conducting research on pollutant emissions resulting from the combustion of candidate fuels. This research, under the direction and sponsorship of the NREL, has primarily been concerned with the combustion of compressed natural gas (CNG), liquefied petroleum gas (LPG), methanol, and ethanol.

In the first 24 months of the current program, studies of the oxygen rich, stoichiometric, and fuel-rich thermal degradation of these fuels in the temperature range of 300 to 1100°C at atmospheric pressure and for reaction times of 1.0 and 2.0 s were completed. Organic products were identified and quantified for each fuel as a function of temperature. The results of these studies agreed well with the results of tail-pipe emission studies in that the types and quantity of emissions measured in both the laboratory and engine tests have been shown to be very similar under certain operating conditions. However, some chemicals were observed in the laboratory study that were not observed in the engine studies and vice versa. This result is important in that it has implications concerning the origin of these emissions. As a result, we have developed a "failure mode", zone theory of the origin of pollutant emissions. The concept is that different pollutants are formed in different zones of the engine-exhaust system. Thus to effectively control emissions we must first know where as well as under what conditions pollutants are formed.

Figure 1.1 presents a simplistic zone model for the origin of pollutant emissions from internal combustion engines that is based on what is known concerning emissions from burning of conventional gasoline.

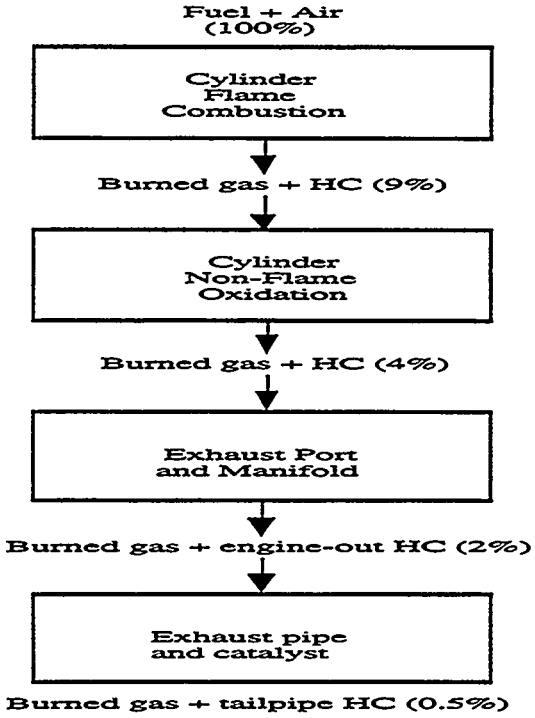

Figure 1.1 Schematic Representation of a Zone Model for the Origin of Automotive Emissions

Only about 91% of the fuel is consumed in the cylinder flame during the power stroke, with 9% of the fuel escaping unburned or converted to products of incomplete combustion (PICs). About 2% of this unburned fraction is decomposed in the exhaust port or manifold following the exhaust stroke and about 5% is decomposed in the cylinder during the subsequent intake or compression strokes. Of the remaining 2%, about 1.97% is degraded in the exhaust pipe or catalytic converter.

The key questions are: 1) how do these proportions change for alternative fuels? and 2) which pollutants are formed in each zone?

Table 1.1 presents the results of a partial, qualitative assessment of these questions. Here we have identified potential engine failure modes, i.e., conditions or zones where combustion may not be complete.

Table 1.1 Failure Mode Analysis

Failure Mode	Indicator	Parameter	Correlation
In-cylinder thermal quenching	Oxidizability	T_{99} (ox)	No
		T_{PIC} (ox)	No
		T_{ad}	Yes
Post-cylinder pyrolysis	Thermal Stability	T_{99} (py)	No
		T_{PIC}(py)	No
Oil layer adsorption	Oil Solubility	H_c, $K_{o/w}$	No
		V.P.	Yes
Crevice wetting	Capillary Action	ξ	Yes
Liquid fuel pooling	Vapor Pressure	V.P.	Yes

We have also identified which fuel properties would control destruction under each failure mode. For example, oxidation kinetics would control emissions from the cylinder under conditions of thermal quenching at the cylinder wall or cooling of the cylinder gas by intake air. Consequently, the oxidizability of the fuel as represented by the temperature required for 99% destruction (T_{99} (ox)); the oxidizability of PICs from the fuel as represented by the temperature of maximum PIC formation (T_{PIC}(ox)); and the burning temperature of the fuel as represented by its adiabatic flame temperature (T_{ad}) are all fuel parameters that might control the efficiency of destruction in the cylinder under thermal quenching. In the post-cylinder regions, oxygen-starved degradation may be dominant. Thus, the pyrolytic stability of the fuel (T_{99} (py)) and the pyrolytic stability of the PICs (T_{PIC}(py)) may control emissions. If the fuel is dissolved in an oil layer then its oil solubility as represented by its Henry's Law constant or octanol-water partition coefficient (H_c and $K_{o/w}$, respectively) or volatility as represented by its vapor pressure (V.P.) may control emissions. If the fuel is in a cylinder groove or crevice, the capillary action as indicated by surface tension (ξ) may control emissions. If liquid fuel pools are formed on the cylinder head, then the vapor pressure of the fuel will correlate with efficiency of destruction. Insufficient data are available to include failure modes associated with the catalytic converter and other exhaust manifold surfaces.

The various fuel properties identified in Table 1.1 were correlated in a rank-order manner with emissions from different alternative fuels. Positive correlations were obtained for the adiabatic burning temperature, vapor pressure as related to oil layer adsorption and liquid pool formation, and surface tension as related to capillary action in cylinder crevices. These correlations suggest that pollutant emissions most likely result from absorption of the fuel in oil layers, wetting of crevices, and thermal quenching of the cylinder or in the exhaust manifold. Reactions on the surfaces of the exhaust system and the catalytic converter are expected to contribute to emissions but were not directly addressed in this series of correlations to due to a lack of experimental data.

The chemical nature of the emissions is also likely to depend upon the failure mode and zone in which the emissions are produced. Our previous flow reactor and elementary reaction kinetic studies indicated that a wide range of types of PICs can be produced. Figure 1.2 presents a breakdown of organic products from the stoichiometric oxidation of six alternative fuels including results from this current study. The nature of the hydrocarbons is as expected and consists of alkanes, olefins, and alkynes. In addition, oxygenates, including alcohols, aldehydes, and ethers were observed. These species can be very reactive and act as efficient ozone precursors. Under

fuel-rich conditions, aromatics and alkylated aromatics were observed and are indicative of molecular growth type reactions that can occur in all combustion sources.

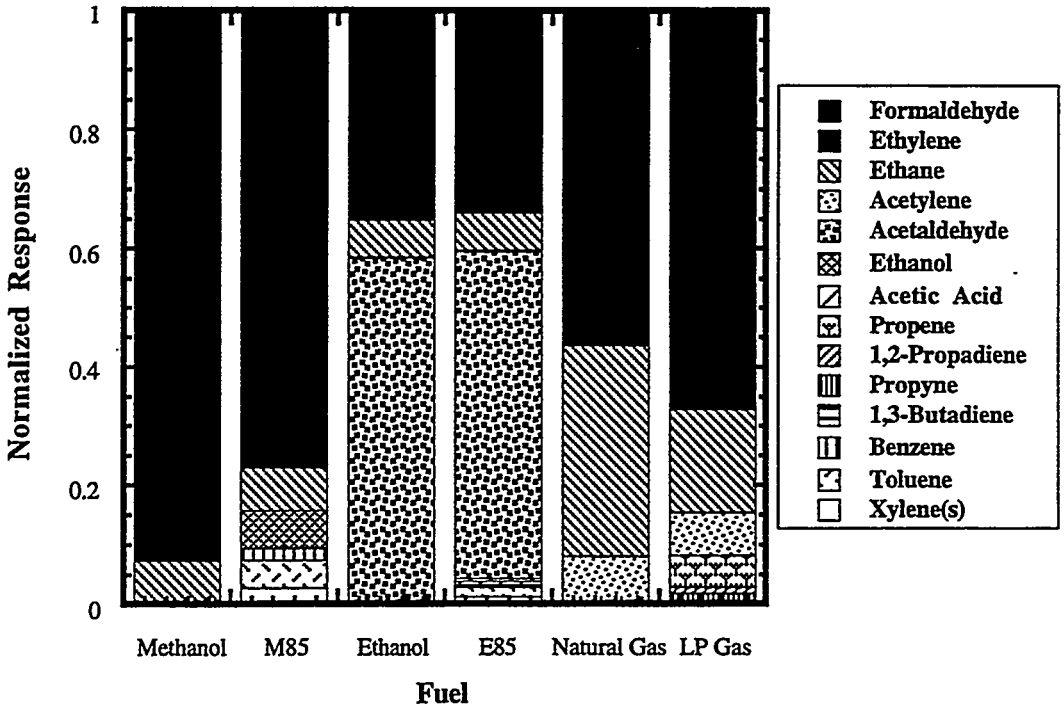

Figure 1.2. Normalized organic emissions from six alternative fuels. Experimental conditions for methanol, M85, ethanol, E85: T_r = 750°C, t_r = 0.75 s. ϕ = 1.0. Experimental conditions for LP Gas: T_r = 850°C, t_r = 0.75 s. ϕ = 1.0. Experimental conditions for Natural Gas: T_r = 1035°C, t_r = 0.75 s. ϕ = 1.0. Benzene, toluene, and the xylene(s) were initial fuel components in M85 and E85.

As a result of our current research, we have identified several questions and issues that are the subject of this report:

1. Why do our flow reactor results obtained at 1 atmosphere and temperatures below 1100°C agree so well with engine tests where the mean pressures are in excess of 5 atmospheres and bulk cylinder temperatures are in the vicinity of 1500°C? The agreement suggests that either the pollutant formation reactions are not very temperature/pressure dependent or that pollutants are not formed as a result of the bulk combustion conditions in the cylinder. Of these two explanations, we favor the latter. Fuel which is adsorbed in oil layers or cylinder crevices experience lower temperature degradation due to the water cooling of the cylinder walls. Thermal degradation reactions can also occur in the cylinder exhaust port and downstream exhaust system at lower temperatures and relatively long reaction times. Our flow reactor studies are expected to reflect the conditions in these engine/exhaust "zones" rather well. The implication is that the mean combustion conditions have little impact on the nature of pollutant emissions and that chemistry occurring in peripheral thermal degradation zones control pollutant formation and emission.

2. What is responsible for the differences in our flow reactor and engines test results? One possibility is that our reaction conditions do not accurately reflect the engine conditions.

However, based on the brief discussion presented in the previous paragraph, other explanations enumerated below are more likely.

a) One variant from engine conditions in our experiments is that our reaction mixture does not contain products of complete combustion in the initial reaction mixture. Specifically, NO_x can effect oxidation of hydrocarbons and alcohols. NO and NO_2 can effect the oxidation chemistry cycle resulting in more hydrocarbon and oxygenated hydrocarbon emissions.

b) A second variant in our studies, is that in the case of methanol and ethanol, we are using pure chemicals instead of real fuels. The hydrocarbon components within these real fuels may significantly effect pollutant formation reaction chemistry and kinetics.

c) A third possibility is that significant pollution formation may be occurring as a result of surface-induced reactions in the exhaust pipe or catalytic converter.

3. How do the measured pollutant emissions from our studies of alternative fuels compare with a baseline case of reformulated gasoline. A controlled scientific study should include a baseline or "control" case. The thermal degradation of reformulated gasoline, recently examined in engine tests by SWRI could suffice as a control. By obtaining data on a baseline fuel, much of the uncertainty concerning the agreement or disagreement between data sets on alternative fuels could be alleviated.

The following sections of the report address these questions. The research is presented by task as defined in the modified statement of work.

Task 7. Baseline Studies of Reformulated Gasoline

Introduction

The wide-scale introduction of reformulated gasolines introduces new aspects to the study of pollutant emissions. With the inclusion of sizable concentrations of MTBE (~10 wt %) in these RFG mixtures, the stable products of incomplete combustion (PICs) are anticipated to be different from conventional gasoline exhaust. Significant analytical capability exists for analyzing emissions that consist of C_{10} hydrocarbons and lower. However, the sheer quantity and complexity of trace-level effluents of C_{11} and higher-molecular-weight organics requires extensive analytical capabilities which involve high-resolution gas chromatography (HRGC) and other elaborate instrumental analysis techniques. In many cases, several of the procedures of separation science need to be involved, such as multi-dimensional GC [1] and various associated instrumental techniques [2], e.g., IR spectroscopy or mass spectrometry.

The analytical methods that exist for analyzing conventional gasolines using HRGC and HRGC-MS have evolved to a high level of performance. Even so, it should be recognized that this advanced analytical capability exists only for the parent fuel [3,4]. It does not necessarily exist for analyzing combustion exhaust samples. The latter type of sample is much more complex, and in many cases, the constituents are of a highly dilute nature within a collected matrix.

Baseline studies of reformulated gasoline are needed to identify those emission components which are different from typical exhaust emissions generated from conventional gasolines. It was anticipated that a significant variety of oxygenated or polar hydrocarbons would be present in the various exhausts from burning RFG samples. The objective of these RFG effluent baseline studies were to identify the polar and higher molecular weight substances that are generated as stable emissions.

Experimental

The approach employed in this task was to subject reformulated gasoline to controlled thermal exposures [5] using our thermal decomposition analytical system (TDAS). A well-defined MTBE-containing RFG sample (designated EM-2060-F; obtained from SwRI; used as-received) was admitted to this system using a syringe pump for steady-state sample injection. Helium gas was used as the diluent for a controlled flow of dry air which had passed through a hydropurge filter. The TDAS was configured in a manner quite similar to that used in recently completed thermal decomposition studies of methanol, ethanol, natural gas, and LP gas [6]. In that research, experiments were conducted under fuel-lean, stoichiometric, and fuel-rich conditions.

A series of high-temperature exposure conditions was established, and samples of the various respective effluents were obtained. Several sample trapping techniques were investigated. Although various sorbent trapping matrices and methods were examined, a procedure was eventually adopted in which the TDAS reactor effluent was bubbled through ice-chilled n-hexane. This procedure was selected as it best interfaced with the subsequent sample processing methods. Also, it has recently been found [7] that normal hexane, although a weak solvent for polar solutes, is the most desirable solvent for performing subsequent HRGC separations and detection using coupled mass spectrometry.

After conducting several experimental screening examinations, it was found that at temperatures below 550°C, there was a preponderance of unburned fuel components captured in the collection vessel. At much higher temperatures (greater than 700°C) only small concentrations of organic effluents were produced. Accordingly, a 600°C temperature was eventually selected, as at this temperature, under stoichiometric conditions, and with a 2.0 s residence time, anticipated levels of PICs were produced. All of the effluent analyses performed in this work were conducted with samples processed under these conditions.

A number of different HRGC technologies were considered for analyzing these collected effluent samples. However, as with various turbine engine fuels and related complex industrial organic waste samples, a significant chromatographic baseline elevation was observed even when using extremely high efficiency open tubular columns (OTCs), see for example Figure 7.1.

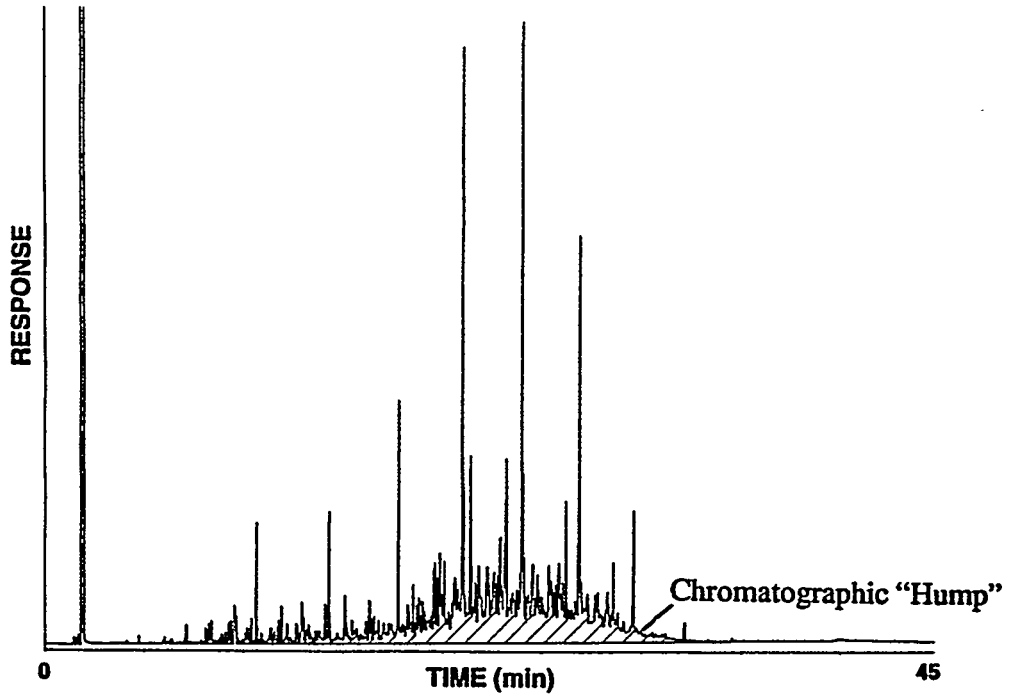

Figure 7.1. Example of baseline elevation in HRGC with highly complex samples.

When such complex samples are subjected to GC-MS, there is considerable difficulty in obtaining high-quality representative spectra of isolated solute zones. In view of the environmental concerns and importance of polar effluent components, it was decided to employ selective fractionation procedures to the collected samples. Accordingly, a silica gel solid-phase extraction (SPE) procedure was used to separate polar compounds from the relatively non-polar matrix. The SPE cartridges (J.T. Baker) contained 1 g of silica gel (SiOH) held in place by polyethylene frits in a 6 ml polyethylene tube. HPLC grade methanol (5 ml) (Fisher Scientific) was used to elute any polar impurities from the adsorbent before the cartridge as used. The silica gel was prepared by adding three 5 ml aliquots of HPLC grade heptane (Fisher Scientific), pulling the solvent through the bed with a vacuum manifold. The heptane activated the porous material in preparation for the sample which followed. The sample was added to the bed in two 5 ml aliquots; all of the polar compounds of the mixture were adsorbed onto the silica gel in this normal phase extraction procedure. A colored band of visible polar compounds could be seen around the top of the silica gel bed. The bed was then washed with 15 ml of heptane to remove the non-polar fuel effluent components, leaving only the heptane and polars in the bed. Finally, methanol was used to elute the polar compounds from the bed. The polar compounds in heptane and methanol were then blown down with dry nitrogen; methanol was then added (200 µl) for injection into the MDGC. The material was concentrated from the collected sample by a factor of 50 (10 ml to 0.2 ml). This particular type of sample was then examined again, by high resolution GC-MS, employing an

especially efficient OTC. Although somewhat lower levels of solute superpositioning were in evidence, it was still necessary to invoke a greater degree of chromatographic resolving power prior to performing mass selective detection.

Our laboratory has had considerable experience [8-11] implementing and working with multi-dimensional gas chromatography (MDGC), and particularly with a technique referred to as MDGC-MS. In its latest operational form [11], a low-temperature trap is included in this instrumental assembly for capturing narrow heart cuts from an initial OTC elution. The contents of this -80°C trap are then re-chromatographed on another OTC of significantly different selectivity. This special analytical assembly (see Figure 7.2) not only produces excellent baselines [9] for performing quantitation of selected solutes, but also permits significantly improved chromatographic separation of solutes so that mass spectral identifications [8,9,11] of individual zones can be accomplished with greater accuracy.

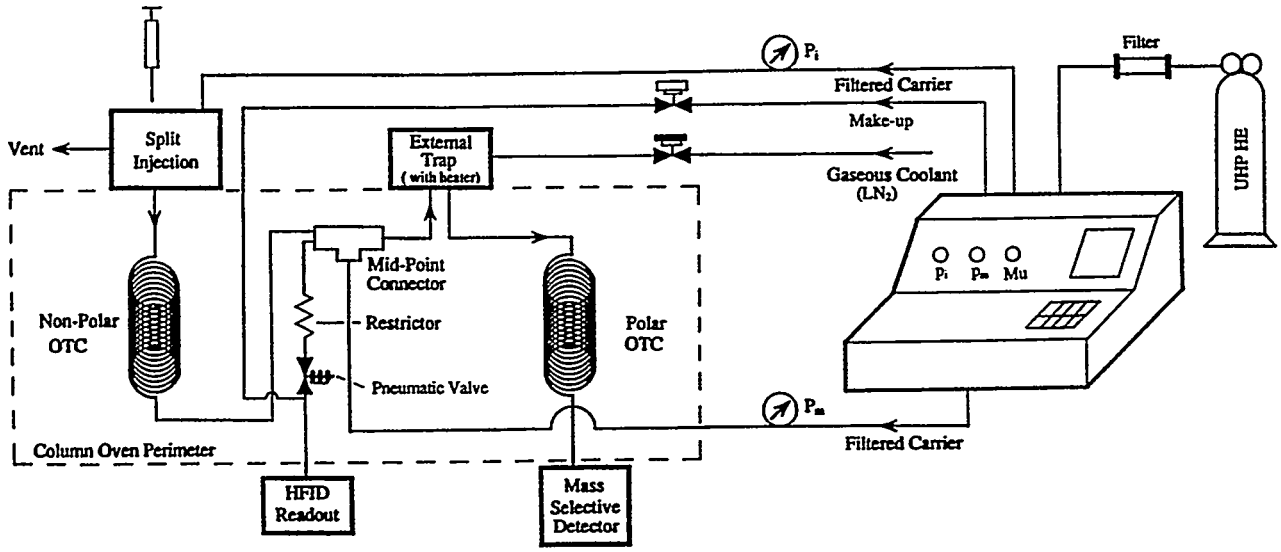

Figure 7.2. Schematic of MDGC-MS System.

A special technique referred to as sequential repetitive heart cutting MDGC [12,13] was employed to obtain a sequential series of segments from the original chromatogram so that each could be subjected to further chromatographic separation and mass selective identification. Although this was a lengthy and time consuming process, it was capable of providing information that could not be readily obtained otherwise. This MDGC-MS assembly, and its sequential heart cutting mode, was the primary analytical method used for conducting the special analyses of RFG effluents.

Instrumental Analysis Data and Results

A variety of GC and MS equipment were used in this study. The conventional GC-MS analyses were performed using a Hewlett-Packard 5890 Series I GC instrument coupled to a HP-5971

MSD. Figure 7.3 shows the resulting GC-MS chromatogram from the solid-phase extract sample. The two marked peaks (or regions) were selected for more detailed mass spectral identification.

This same sample was then subjected to MDGC-MS analysis. Figure 7.4 shows the resulting two chromatograms obtained after splitless injection of a 2.0 microliter sample. The upper tracing in this figure represents the chromatogram produced by a 30 m by 0.25 mm by 0.25 μ 5% phenylmethylsilicon phase column. The lower tracing is the recorded output from that same column when two heart cuts were obtained for subsequent separation using a moderately polar 1701 cyanosiloxane phase OTC of the same physical dimensions as the initial column. The two heart cuts were trapped at temperatures lower than -80°C and the output from the mass spectrometer is shown in the upper tracing in Figure 7.5. The lower tracing was a typical blank sample that was previously generated on this particular instrumental assembly. It is seen that what constituted a doublet in the upper chromatogram of Figure 7.4b is now many solute zones which can be quantitated, and more importantly, easily identified because of the very good baseline (or zero reference level) that is presented to the mass spectrometer. This is seen more clearly in the chromatogram of heart cut A and the mass spectrum shown in Figure 7.6.

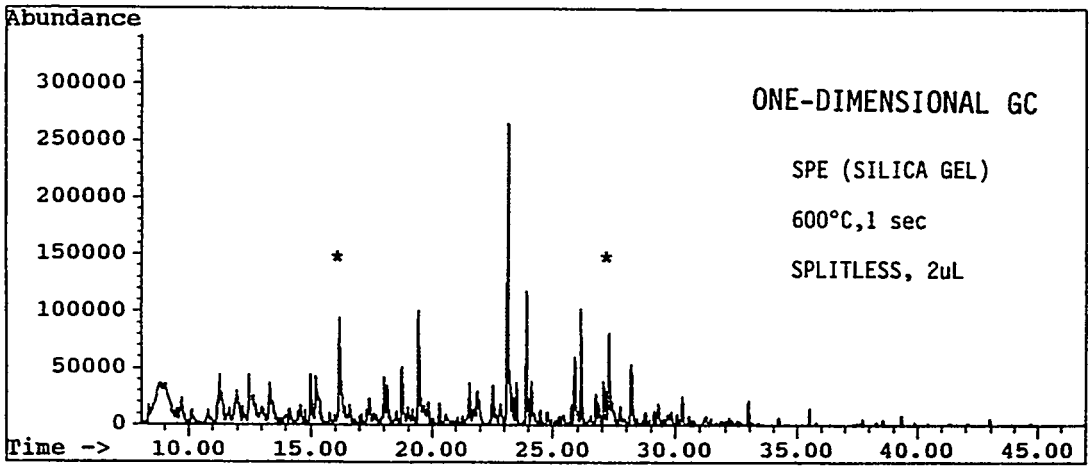

Figure 7.3. Output of conventional GC-MS of RFG effluent subjected to solid-phase extraction.

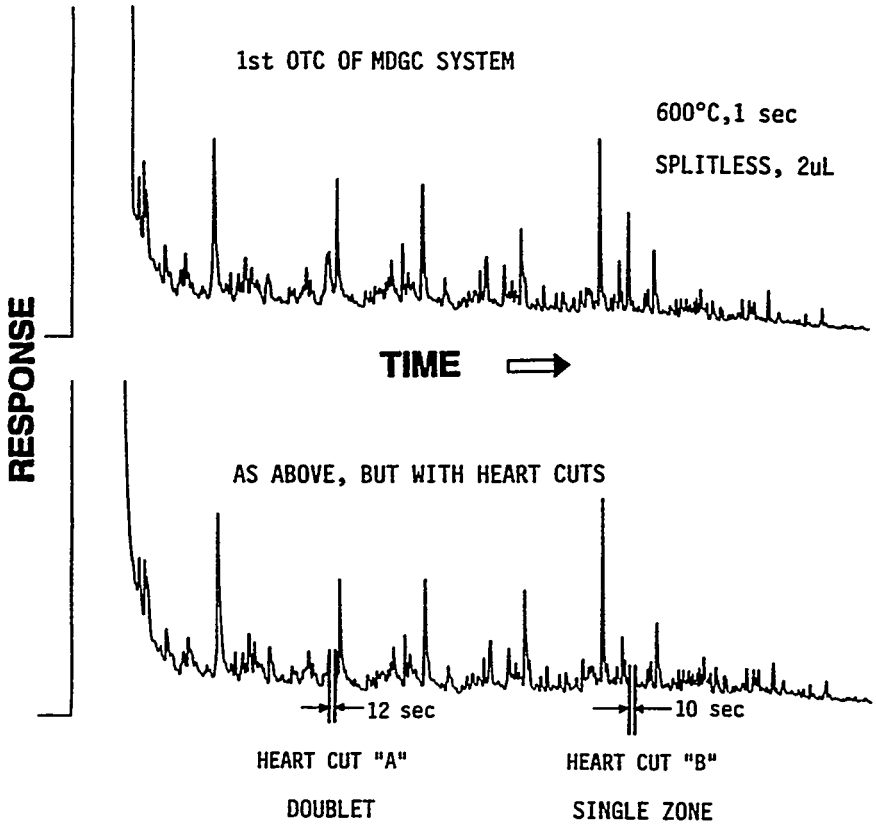

Figure 7.4. Primary channel response using MDGC-MS of RFG effluent subjected to solid-phase extraction.

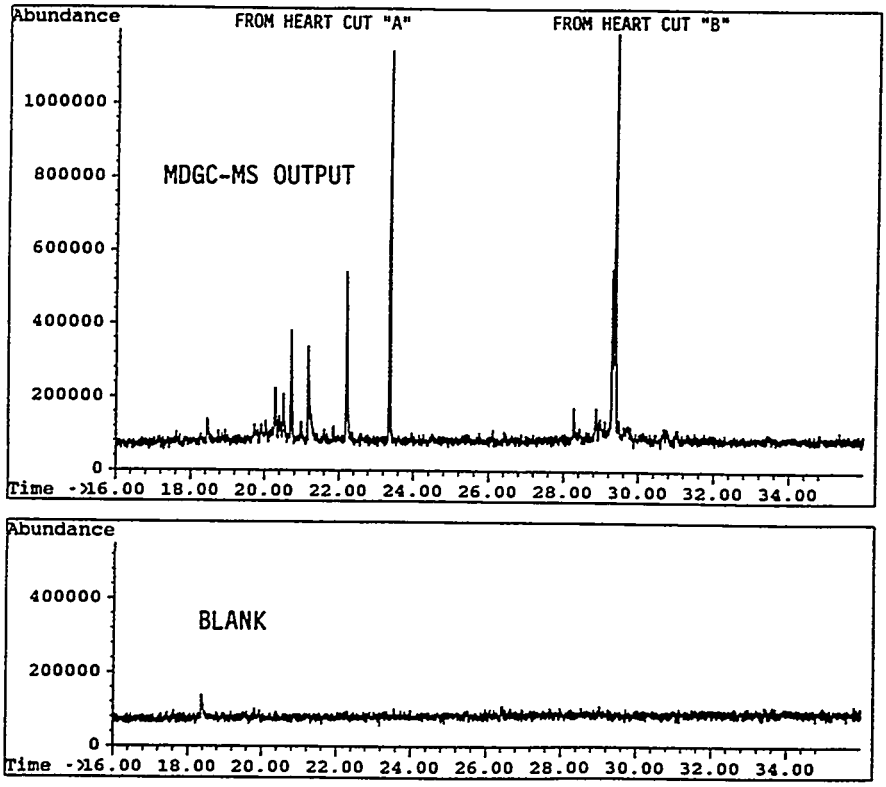

Figure 7.5. MDGC-MS output signals for heart cuts A and B (above) and for instrument blanks (below).

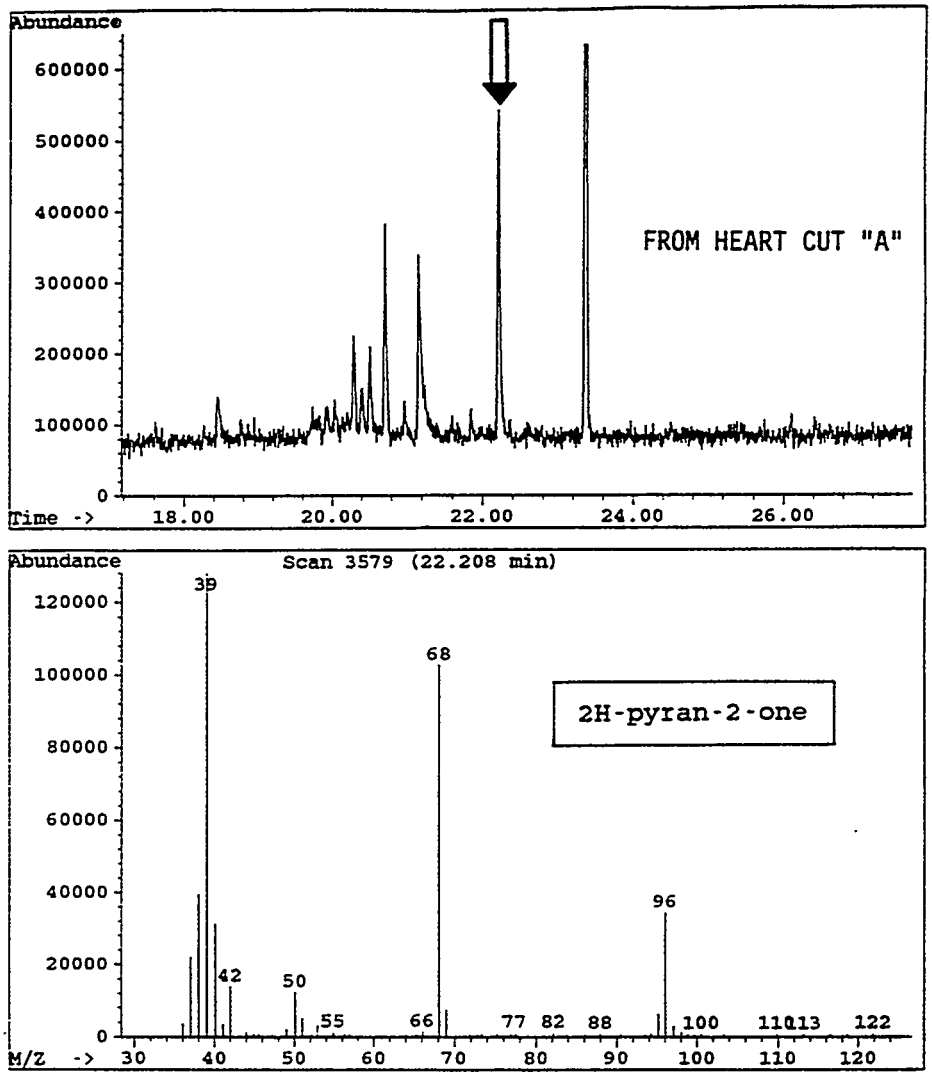

Figure 7.6. GC output and mass spectrum of 2H-pyran-2-one from heart cut A.

A close examination and counting of solutes, as shown in Figure 7.7, revealed there to be at least 18 solutes produced from the previous doublet that was shown in Figure 7.4. Also, Figure 7.8 shows the analysis of heart cut B, where greater than 12 solute zones are now in evidence from the single zone that was heart cut from the chromatogram of Figure 7.4.

Sequential repetitive heart cutting has been used for many years [12], and a refined operational version has been previously proposed by us [13]. This sequential repetitive heart cutting mode of conducting MDGC-MS investigations is a powerful technique for obtaining more detailed analytical information throughout various regions of an entire chromatogram. Essentially, this sequential procedure consists of first selecting a region of a complex primary chromatogram which needs further or more detailed examination. If more than one region is of interest, they must be displaced in time so that there is not a serious overlap of data during the re-chromatographing of the two or more separate heart cuts. In some cases, even three different regions within a complex primary chromatogram could be investigated in this manner.

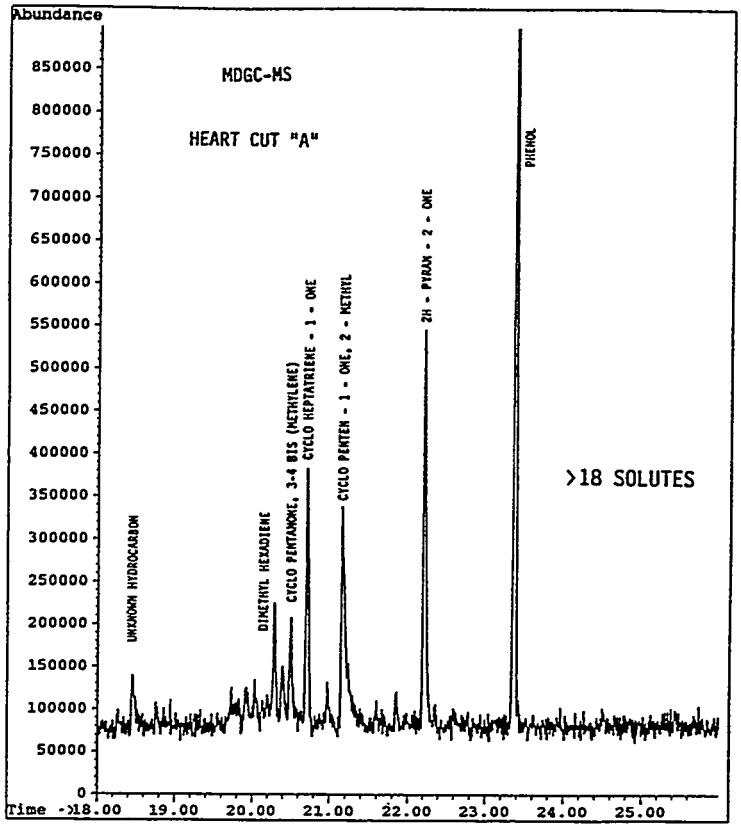

Figure 7.7. Product identifications from MDGC-MS output signal for heart cut A.

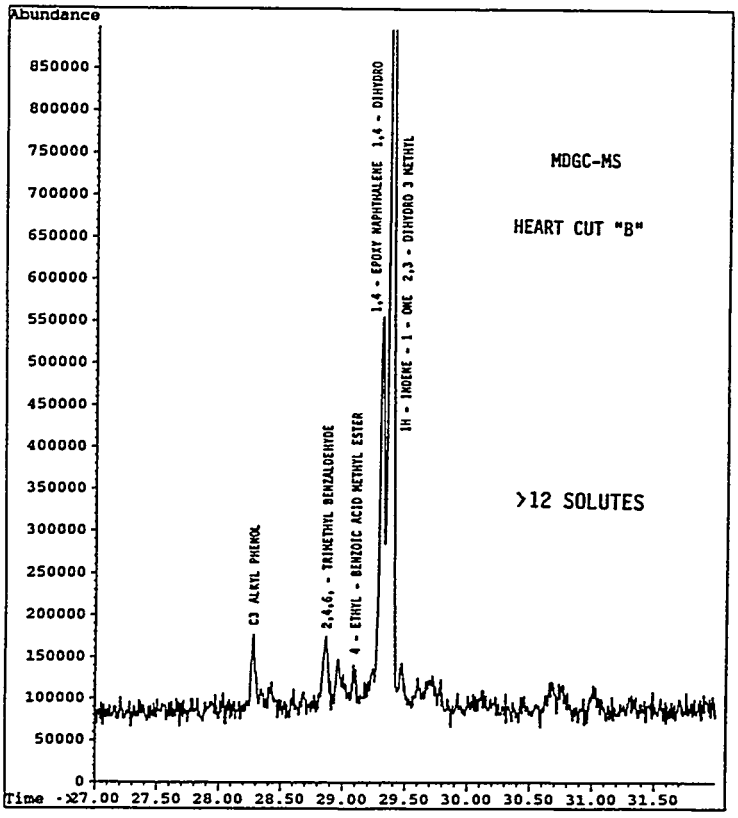

Figure 7.8. Product identifications from MDGC-MS output signal for heart cut B.

The next step is to obtain narrow heart cuts at the start of each selected extended region (see Figure 7.9). Our MDGC approach has always been to obtain narrow heart cuts [9-11] as opposed to the much wider heartcutting practices used by other investigators [12]. Our view is that the time-based width of a heart cut should be no wider than the baseline level width of a typical solute zone (e.g., 10 s wide) as encountered in the primary chromatogram. Large concentration zones that exhibit tailing would exceed the 10 s heart cut width. After the output data are obtained for the first set of heart cuts for the extended regions, the next step is to re-inject the sample and advance to the next heart cut(s) along the time axis of the primary chromatogram. In short, the starting time for the second set of heart cuts is the ending time of the previous 10 s heart cut. This procedure is continued until the entire extended region(s) has been traversed. Using this sequential repetitive heart cutting technique, entire regions of a complex initial chromatogram can be more thoroughly analyzed using MDGC-MS procedures.

By employing the sequential repetitive heart cutting procedure, more than 20 ten-second wide heart cuts were made from extended regions I and II (see output data in Figures 7.9 through 7.18) and a plethora of compounds were identified in this original sample. A listing of many of those tentatively identified compounds is given in Table 7.1. These identifications were accomplished using the NIST mass spectral library and manual mass spectral interpretation.

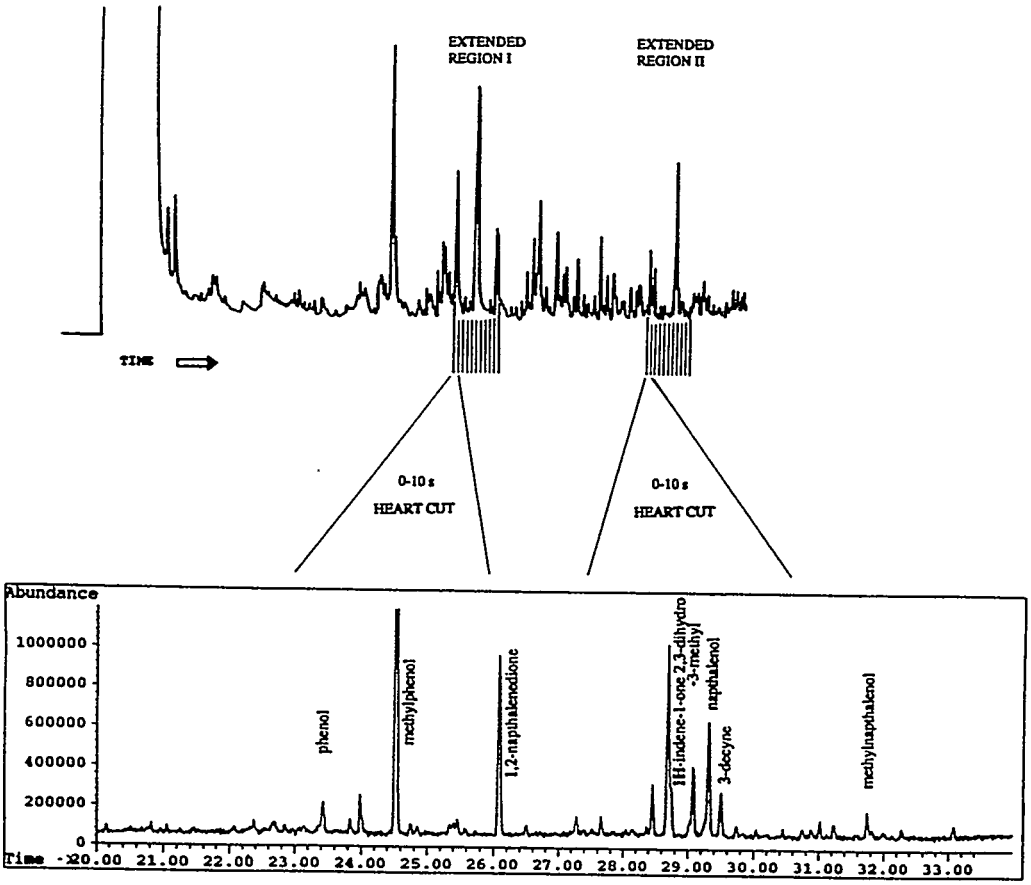

Figure 7.9. Output of sequential repetitive heart cutting MDGC-MSD operation. Data for 0 to 10 s heart cuts.

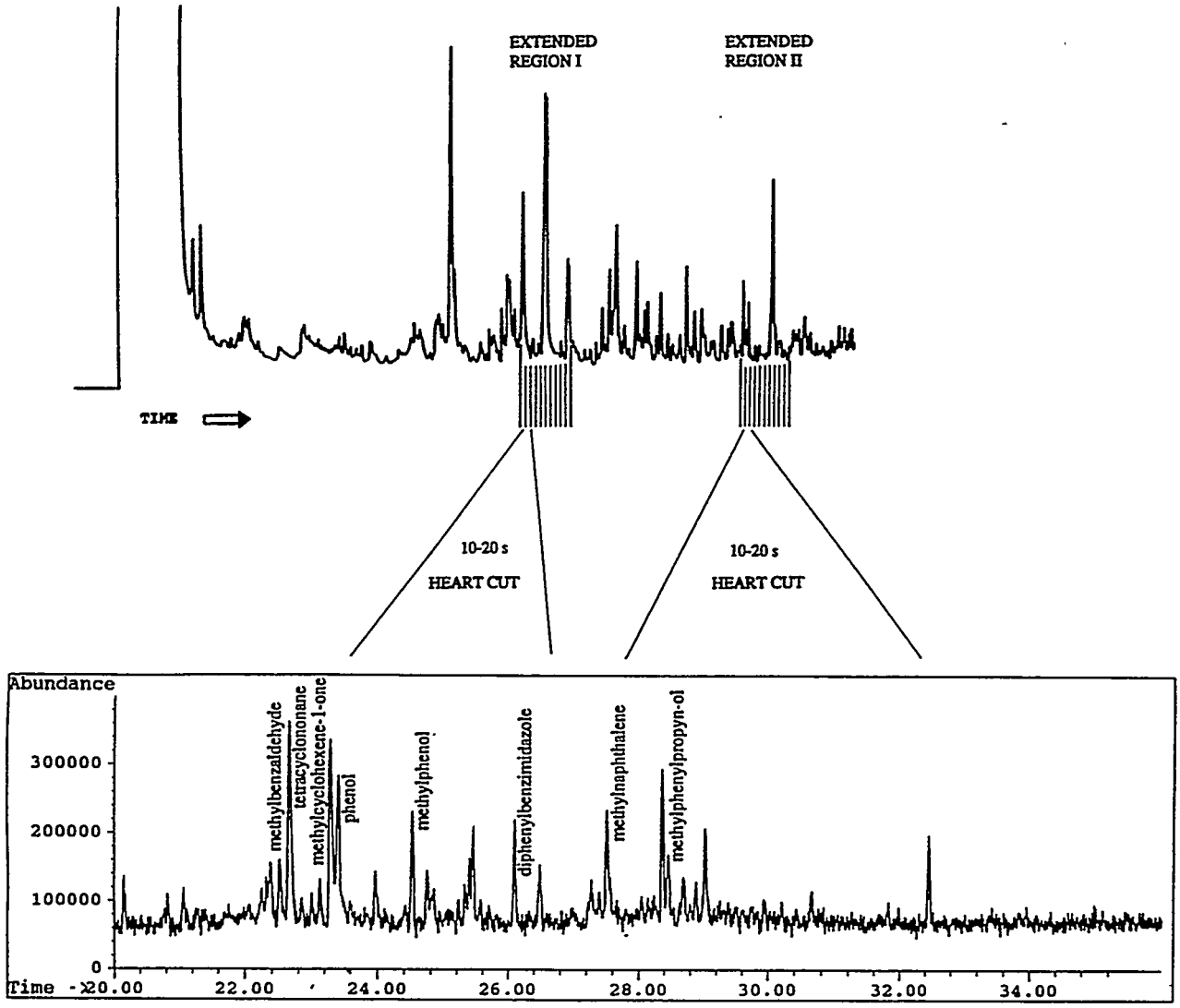

Figure 7.10. Output of sequential repetitive heart cutting MDGC-MS operation. Data for 10 to 20 s heart cuts.

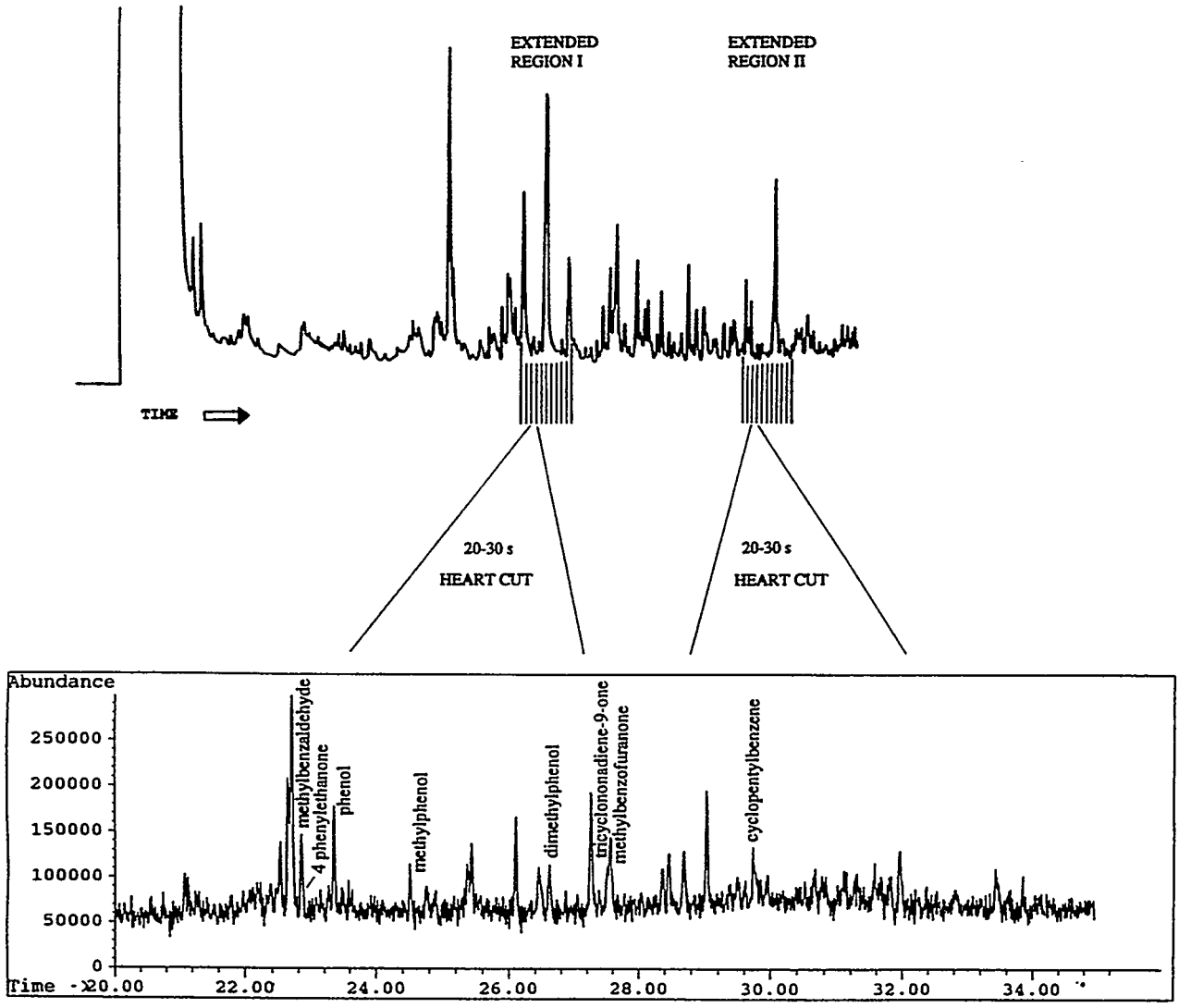

Figure 7.11. Output of sequential repetitive heart cutting MDGC-MS operation. Data for 20 to 30 s heart cuts.

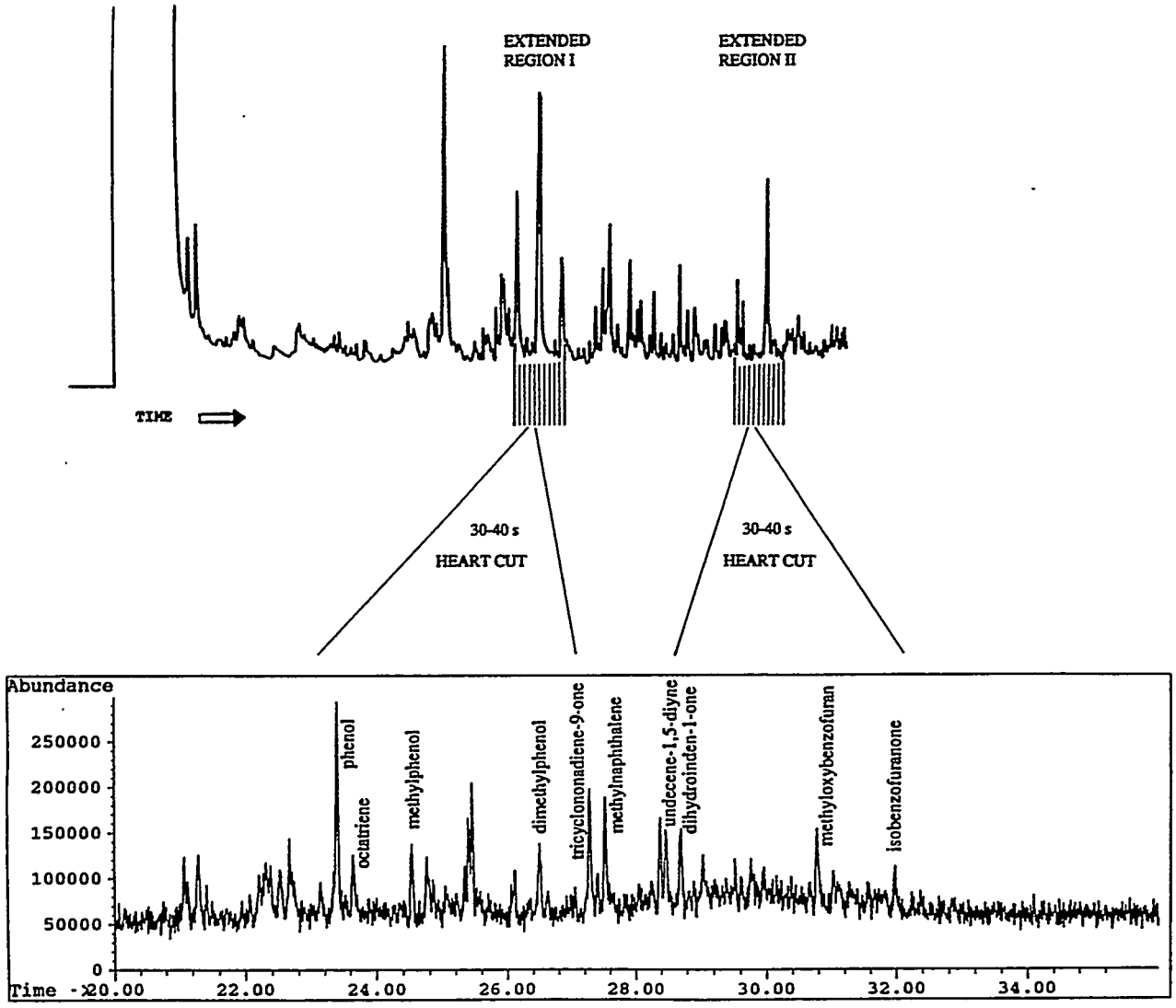

Figure 7.12. Output of sequential repetitive heart cutting MDGC-MS operation. Data for 30 to 40 s heart cuts.

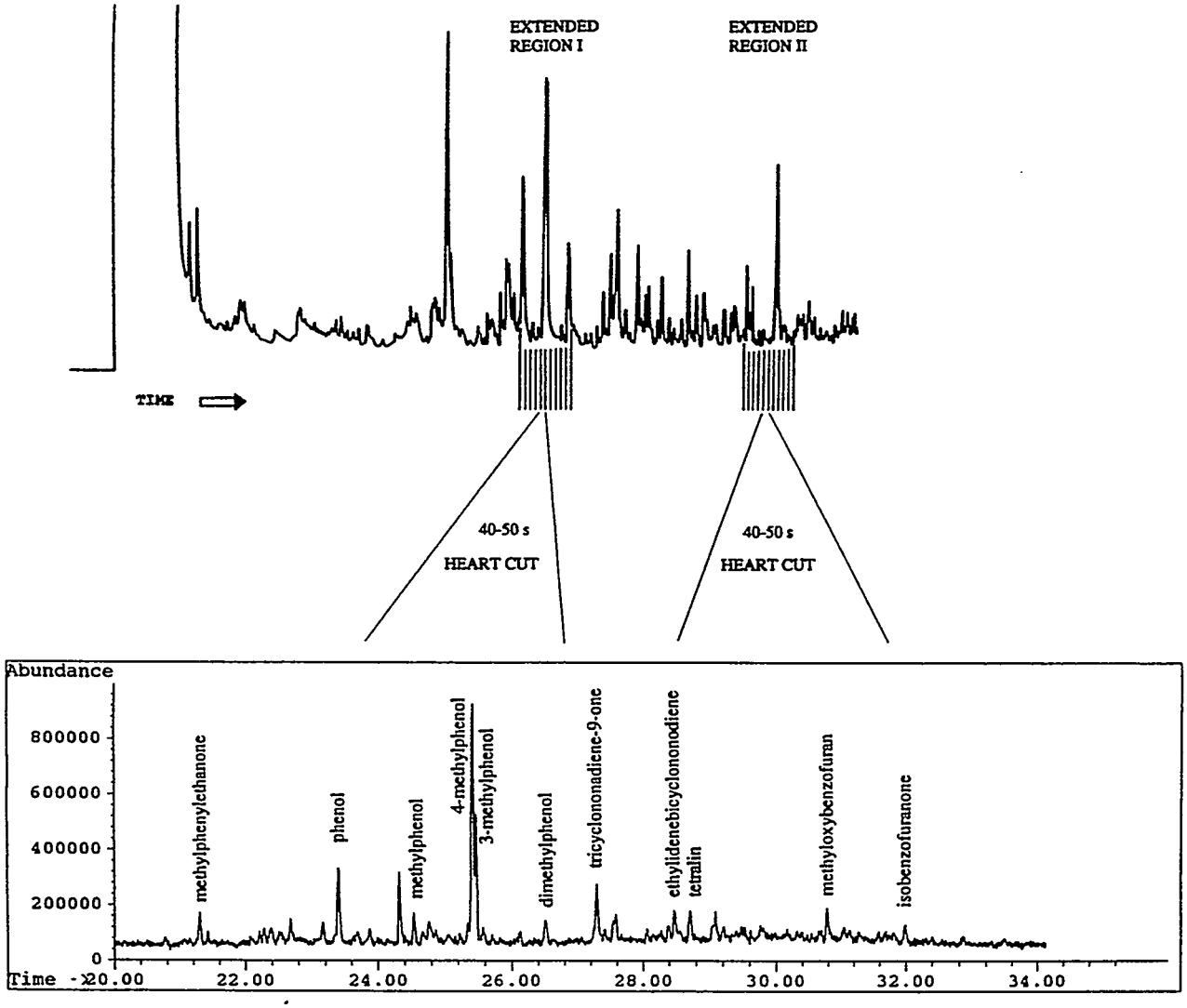

Figure 7.13. Output of sequential repetitive heart cutting MDGC-MS operation. Data for 40 to 50 s heart cuts.

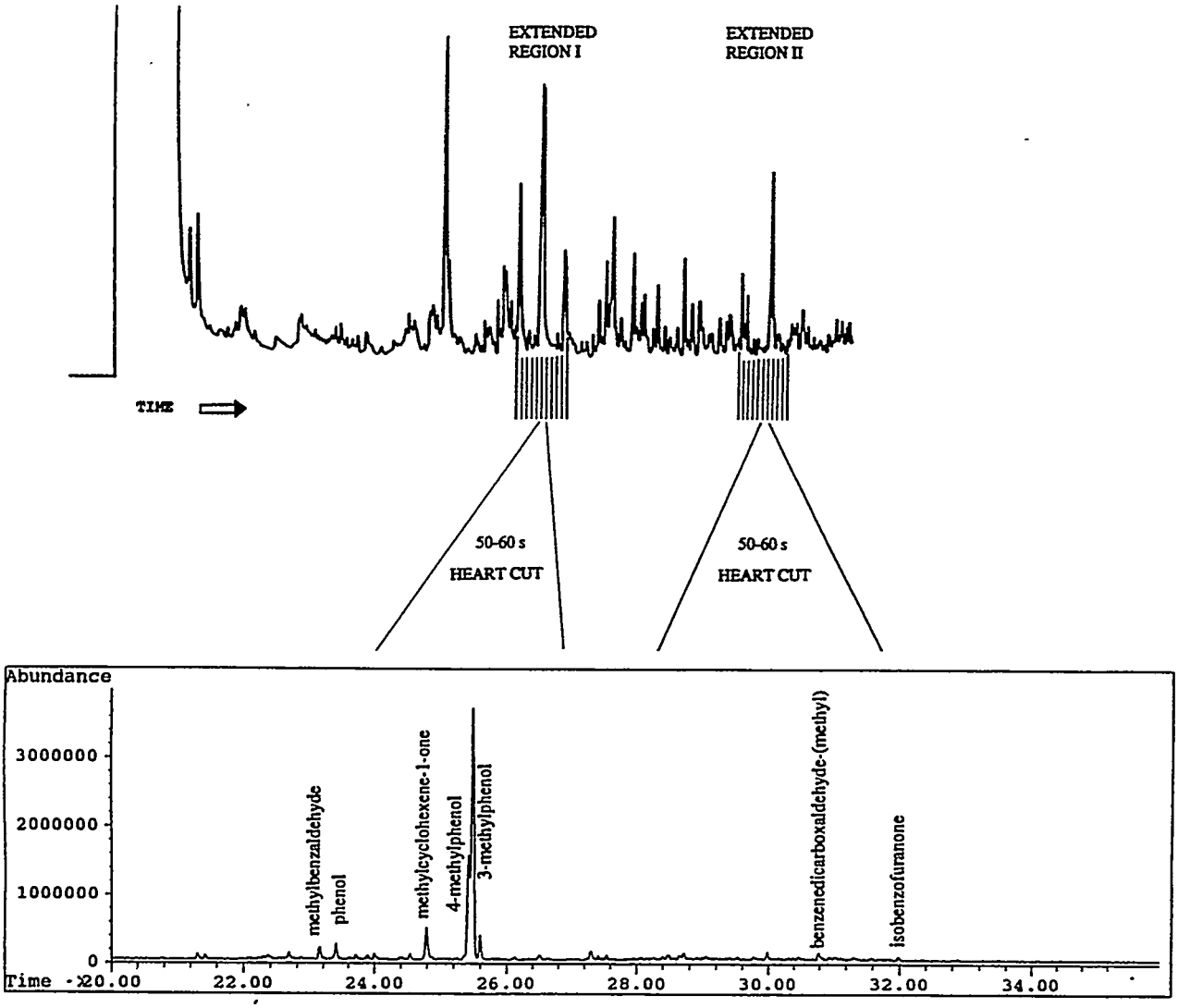

Figure 7.14. Output of sequential repetitive heart cutting MDGC-MS operation. Data for 50 to 60 s heart cuts.

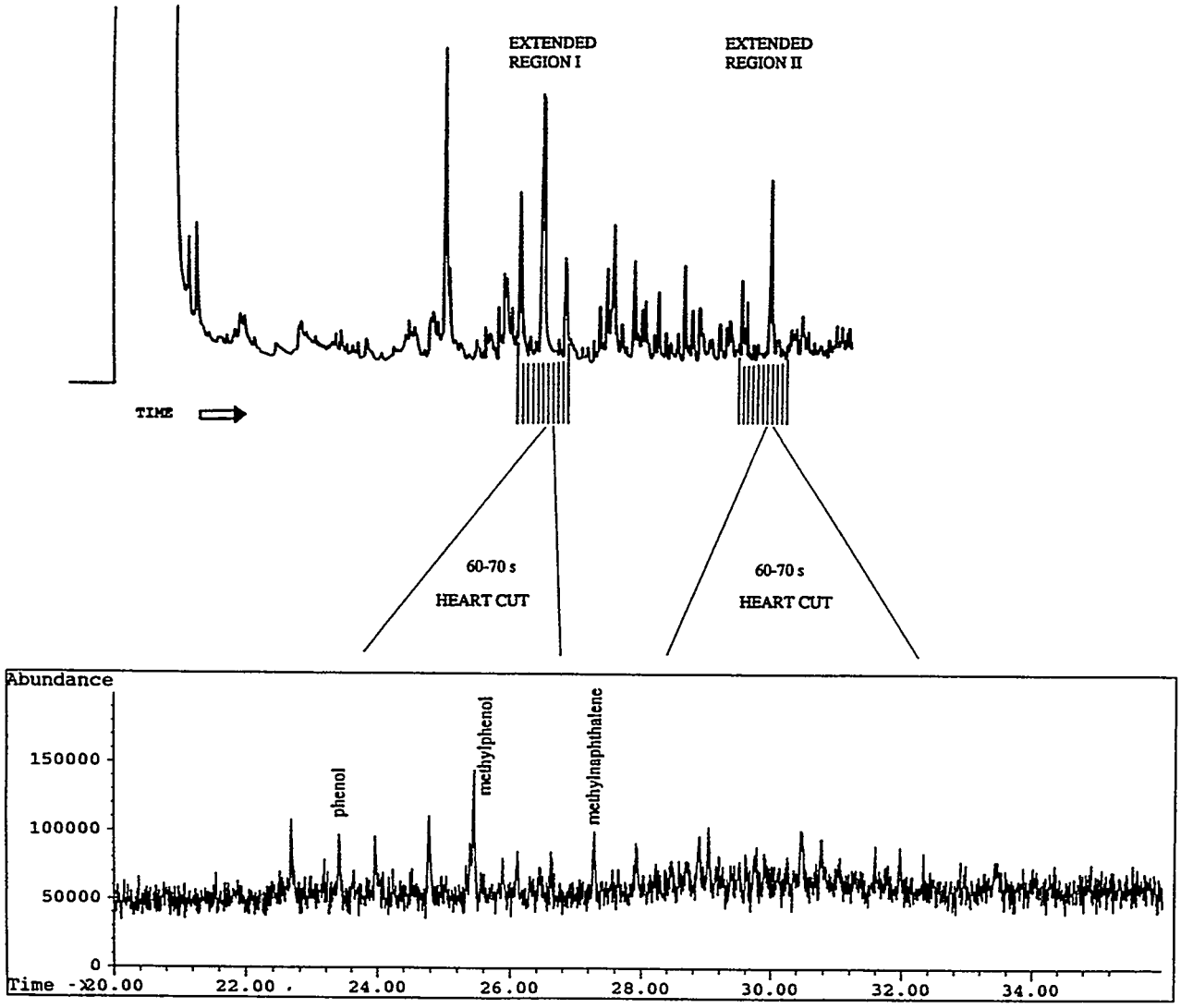

Figure 7.15. Output of sequential repetitive heart cutting MDGC-MS operation. Data for 60 to 70 s heart cuts.

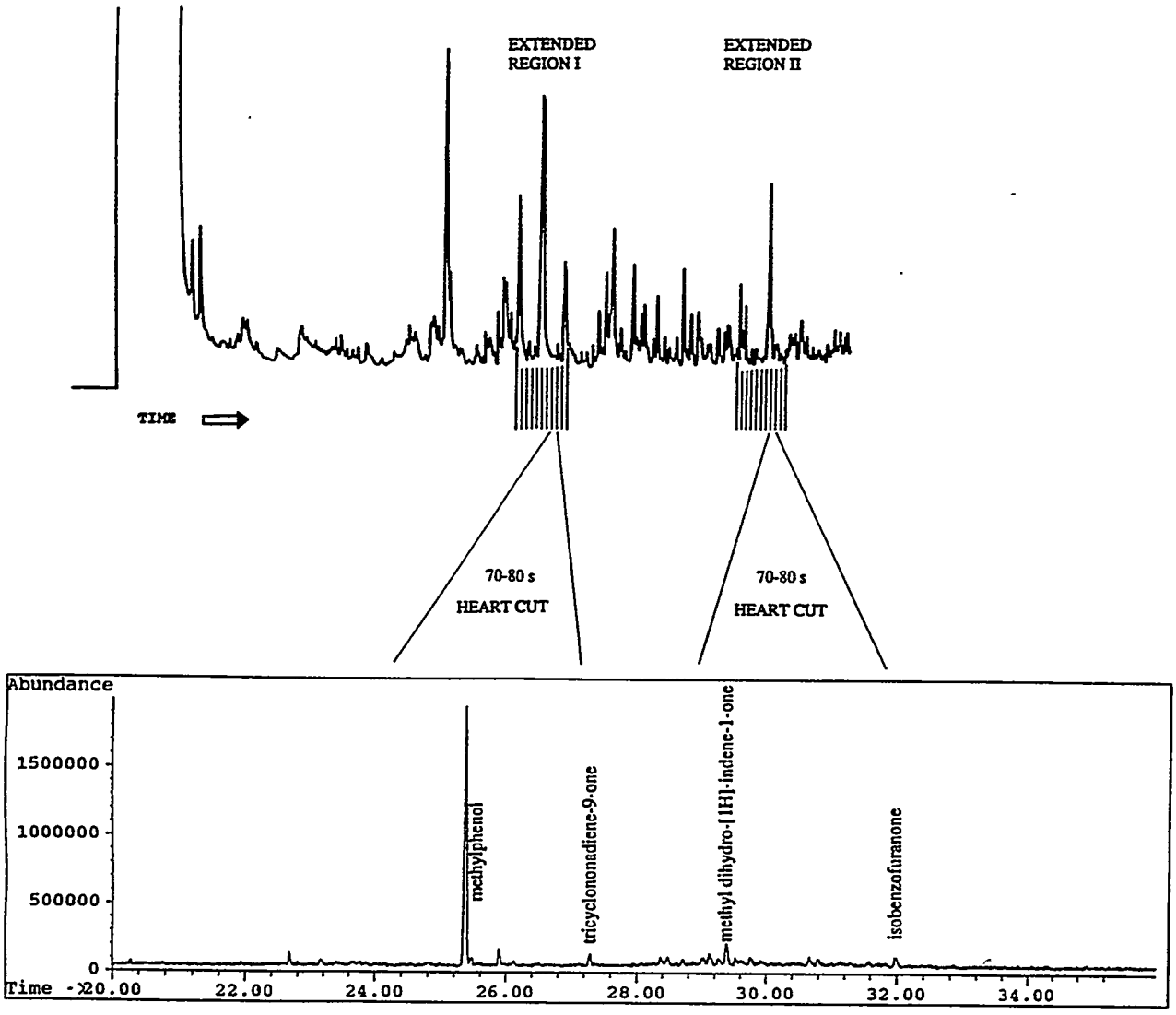

Figure 7.16. Output of sequential repetitive heart cutting MDGC-MS operation. Data for 70 to 80 s heart cuts.

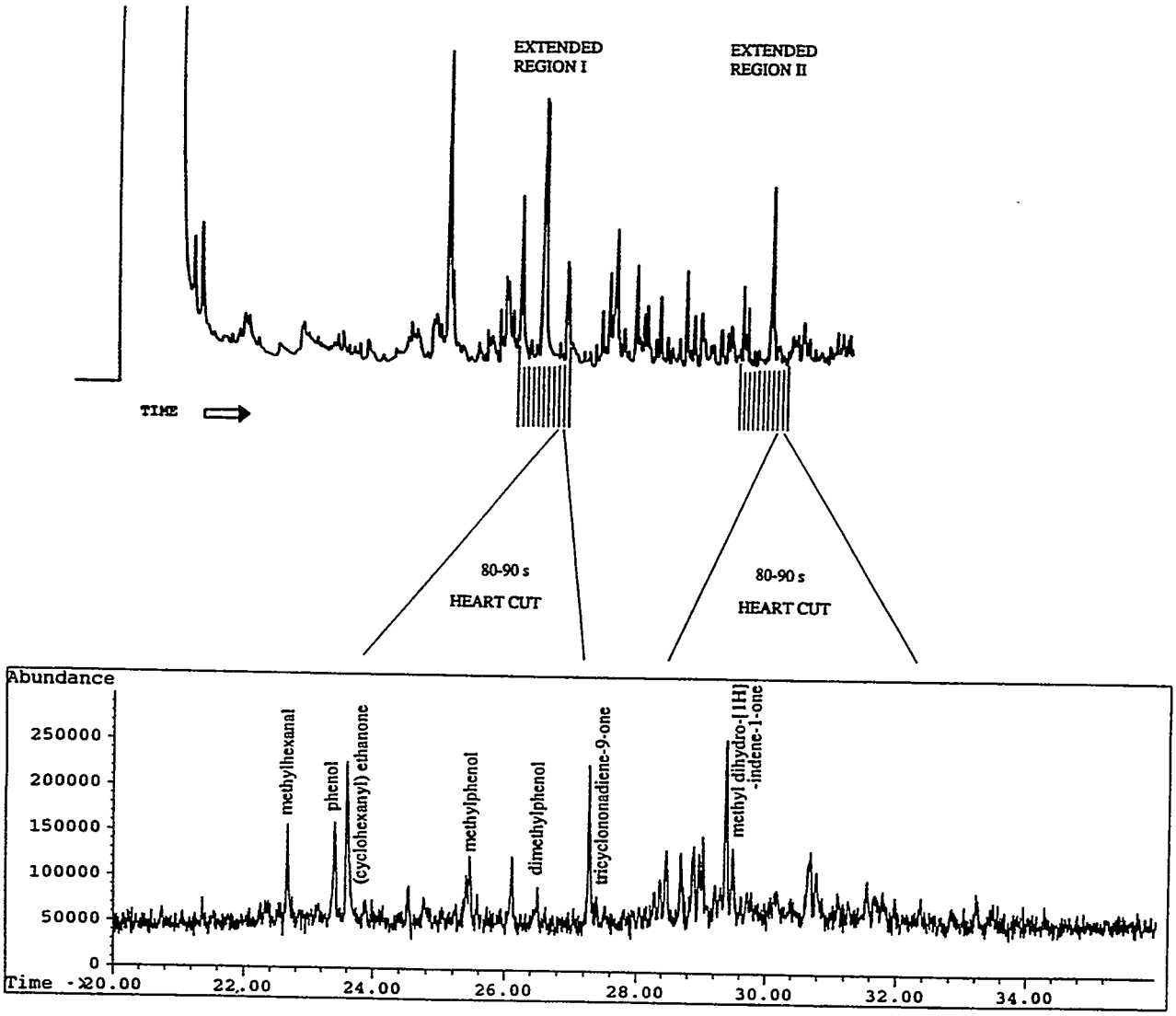

Figure 7.17. Output of sequential repetitive heart cutting MDGC-MS operation. Data for 80 to 90 s heart cuts.

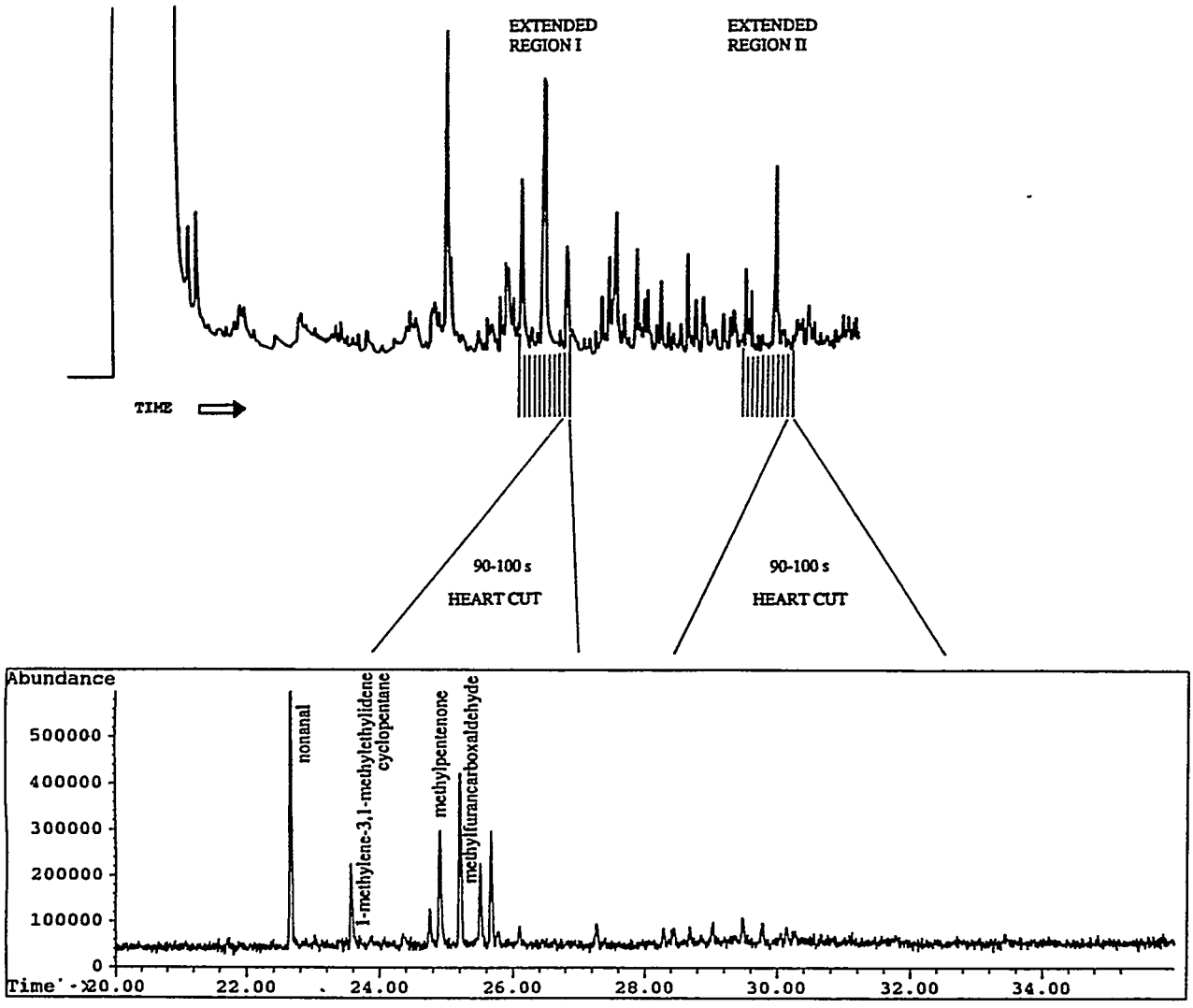

Figure 7.18. Output of sequential repetitive heart cutting MDGC-MS operation. Data for 90 to 100 s heart cuts.

Table 7.1. A Listing of Tentatively Identified RFG Constituents and Associated Oxidation Products after Solid-Phase Extraction and MDGC Analysis

dimethylhexadiene*	propylbenzene*
cyclo pentanone, 3-4 bis(methylene)	3-methyl-3-penten-1-yne
cyclo penten-1-one, 2-methyl	octatriene
2H-pyran-2-one	undecene-1,5-diyne
2,4,6-trimethylbenzaldehyde	dihydroinden-1-one
4-ethylbenzoic acid, methyl ester	isobenzofuranone
1,4-epoxy naphthalene, 1,4-dihydro	methylphenylethanone
1H-indene-1-one 2,3-dihydro-3-methyl	4-methylphenol
methylphenol	3-methylphenol
phenol	2-methylphenol
1,2-napthalenedione	tricyclononadiene-9-one
napthalenol	ethylidenebicyclononodiene
methylnapthalenol	tetralin
methylbenzaldehyde	methyloxybenzofuran
tetracyclononane	butylbenzene*
methylcyclohexene-1-one	trimethylfuran
diphenylbenzimidazole	benzenedicarboxaldehyde-(methyl)
methylnaphthalene*	methylpentenone
methylphenylpropyn-ol	methylfurancarboxaldehyde
trimethylcyclo-penten-1-one	1-methylene-3,1-methylethylidenecyclopentane
4 phenylethanone	nonanal
dimethylphenol	methylhexanal
tricyclononadiene-9-one	(cyclohexanyl) ethanone
methylbenzofuranone	methyl dihydro-[1H]-indene-1-one
cyclopentylbenzene*	3-decyne*

* Initial RFG component.

Discussion

During the course of conducting these thermal decompositions with RFG samples and detailed chemical analyses of their effluent, it was apparent that the exposure temperature at which various PICs are formed is especially sensitive. This type of behavior has been found previously in extensive thermal decomposition tests with various halogenated organic materials [14,15], such as pesticides, PCBs, PBBs, and various industrial organic waste mixtures.

The stability of the formed PICs from RFG starting materials is also of interest. It was noted throughout the extended MDGC-MSD analytical work that the composition of the concentrated extract was changing slightly, even though the sample had been properly stored in the dark to avoid light-sensitive reactions. It can be concluded that some of these partially oxidized organic substances are labile and continued long-term reactions are occurring even at ambient conditions. Again, this is not too surprising as many thermal decomposition products formed from complex PIC matrices, such as liquefied coal [16], also continue to change in composition and concentration over an extended period of time.

A major observation during the course of conducting this research was the intriguing nature of the various PICs. A majority of these compounds, particularly the polar oxygenated species, have not been identified before as combustion effluents from engine tests of reformulated gasoline [17,18]. Analyses from engine tests are typically limited to hydrocarbon species (C_1-C_{12} compounds) and light oxygenates (C_1-C_7 compounds). Also, of keen interest is the potential impact of such PICs

with respect to environmental interactions and toxicological effects [19]. Indeed, very little is known about the behavior of these types of compounds in the biosphere.

In light of the formation of various polar or oxygenated hydrocarbons [20,21] and their associated environmental concerns, it would seem appropriate to investigate more fully their formation from actual automotive vehicle exhaust systems. The concentrations and distributions of such compounds generated should be of considerable interest as their yields, or extent of generation, would seemingly vary with different cycles of automotive operation. Appropriate exhaust sampling techniques can certainly be developed for obtaining such samples, and the analytical methodology is in place at the University of Dayton to perform such investigations.

References

1. Cortes, H.J. 1990. Multidimensional Chromatography: Techniques and Applications, Marcel Dekker, New York.
2. Hirschfeld, T. 1980. Anal. Chem., 52, 297A.
3. Sanders, W.N., and Maynard, J.B. 1968. Anal. Chem., 40, 527.
4. Berger, T.A. 1996. Chromatographia, 42, 63.
5. Rubey, W.A., and Carnes, R.A. 1985. Rev. Sci. Instrum., 56, 1795.
6. Taylor, P.H., Rubey, W.A., Shanbhag, S., Rahman, M., and Dellinger, B. 1995. The Origin and Fate of Organic Pollutants from the Combustion of Alternative Fuels. NREL/TP-425-7607, Golden, CO: National Renewable Energy Laboratory.
7. Grob, K., and Artho, A. 1990. J. High Resol. Chromatogr., 13, 803.
8. Rubey, W.A. 1985. Multidimensional High-Resolution Gas Chromatographic Investigation of Hydrocarbon Fuels and Various Turbine Engine Fuel Precursors, Technical Report AFWAL-TR-85-2033, U. S. Air Force Wright Laboratory.
9. Rubey, W.A., Mazer, S.L., Hayes, P.C., and Steward, E.M. 1986. Analysis of Turbine Engine Fuels and Complex Industrial Organic Mixtures using a Multidimensional GC and GC-MS System, Paper presented at Pittsburgh Conference, Atlantic City, NJ.
10. Rubey, W.A., Taylor, P.H., Striebich, R.C., and Dellinger, B. 1996. Investigation of Reformulated Gasoline Emissions using Multidimensional Gas Chromatography-Mass Selective Detection (MDGC-MSD), Presentation at 26th International Combustion Institute Symposium, Naples, Italy.
11. Anderson, S., Garver, J., Rubey, W., Striebich, R., and Grinstead, R. 1995. The Separation and Identification of Trace Heteroatomic Species in Jet Fuel by Sample Enrichment and Multidimensional Gas Chromatography with Mass Selective Detection (MDGC-MSD), Proceedings of 17th ISCCE, Wintergreen, VA.
12. Gordon, B.M., Uhrig, M.S., Borgerding, M.F., Chung, H.L., Coleman, W.M., Elder, J.F., Giles, J.A., Moore, D.S., Rix, C.E., and White, E.L. 1988. J. Chromatogr. Sci., 26, 174.
13. Mazer, S. 1986. MDGC Automation Successive Heartcutting, Internal Report, University of Dayton.
14. Dellinger, B., Torres, J.L., Rubey, W.A., Hall, D.L., Graham, J.L., and Carnes, R.A. 1984. Hazardous Waste, 1, 137.
15. Graham, J.L., Hall, D.L., and Dellinger, B. 1986. Env. Sci. Technol., 20, 703.
16. Bertsch, W., Anderson, E., and Holzer, G. 1976. J. Chromatogr., 126, 213.
17. California Air Resources Board. 1994. "Preliminary Reactivity Adjustment Factors," Mobile Sources Division, El Monte, CA.
18. Whitney, K.A. 1995. "Determination of Alternative Fuels Combustion Products," NREL/TP-425-7528, Golden, CO: National Renewable Energy Laboratory.
19. Colborn, T., vom Saal, F.S., and Soto, A.M. 1993. Environ. Health Perspect. 101, 378.
20. Levy, J.M., Wolfram, L.E, and Yancey, J.A. 1983. J. Chromatogr., 279, 133.
21. Verga, G.R., Sironi, A., Schneider, W., and Frohne, J.C. 1988. HRC & CC, 11, 248.

Task 8. The Effect of NO_x on the Combustion of Alternative Fuels

Introduction

The objective of this project was to determine the impact of NO_x on organic pollutant formation from the combustion of alternative fuels. Our initial studies used mixtures of oxygen and helium as the reaction atmosphere for the oxidation of alternative fuels. In this task, we have modified this mixture with the addition of NO at levels that would be produced in a spark ignition, internal combustion engine. This study is especially relevant to pollutant formation in the cylinder exhaust port where cylinder NO_x and unburned fuel are mixed and can still undergo reaction at elevated temperatures. This study will also help to determine if any of the observed differences in the our flow reactor studies and dynamometer tests are due to the presence of NO_x in engine tests.

Background

The oxidation of NO to NO_2 in the presence of oxygen has been shown to be strongly promoted, at temperatures as low as 300°C, by the presence of low concentrations of hydrocarbons, CO and H_2 [1-4]. At the same time, the oxidation of the hydrocarbon is greatly sensitized, resulting in the formation of oxygenated species, such as aldehydes and unsaturated hydrocarbon compounds.

Emissions of NO_2 from combustion appliances such as gas cookers and heaters [5] and gas turbines [6] are likely the result of these reactions. It has also been demonstrated [3] that trace concentrations of NO (as little as 0.02 ppm, similar to that often found in urban air) have a profound effect on the oxidation of n-butane. This result suggests that hydrocarbon-NO interactions may also be important in experimental studies of low temperature ignition and in ignition phenomena in automotive engines.

The ability of hydrocarbon fragments such as CH, CH_2 and possibly CH_3, to reduce NO to HCN is employed in "reburning", or fuel staging, when hydrocarbons are injected into hot combustion gases. The subsequent re-oxidation of HCN (and the injected hydrocarbon) results, under appropriate conditions of air/fuel ratios, in substantial formation of N_2, and thus leads to a net reduction in the overall NO emissions. While the reburning process is generally carried out at high temperature, similar interactions could be expected if reactive hydrocarbon fragments were available at lower temperatures.

Evidence for the reburning process at relatively low temperatures (500 to 800°C) has recently been demonstrated in flow reactor studies using a reactant mixture consisting of 1000 ppm C_3H_8, 350 ppm NO, and 2.25% O_2 [7]. Experiments indicated that NO concentrations dropped by 32% with an accompanying increase in the NO_2 concentration. Besides NO_2, another nitrogen-containing species was detected. FTIR spectra analysis established the identity of the species as HNCO. The results provided evidence for hydrocarbon-NO interactions at low temperatures which result in the formation of species containing C-N bonds. The formation of HNCO is of particular interest given its high toxicity which could have substantial impacts on the use of hydrocarbons in NOx reduction technologies and on air quality.

Reburning reactions are thought to proceed through reactions of the general type:

$$CH_i + NO \Longrightarrow \text{products (e.g. HCN, CN, ...)} \qquad \text{(R7.1)}$$

where i = 0-3. Although the rates of the most important of these reactions are now known reasonably well [8], inadequate information is presently available for the product branching ratios. Recently, for example, the reaction between CH_2 and NO was shown [9] to proceed through formation of the addition complex CH_2NO; rearrangement or reaction of this complex to form HNCO may be possible.

Thus, there is considerable justification for both experimental and modeling studies of reactions between hydrocarbons and NO, in the presence of O_2, for the temperature range of 300 to 800°C. Previous work has concentrated on both low concentrations of NO (<100 ppm), typical of those found in household appliances and/or gas turbines [3] and somewhat higher concentrations (~350 ppm) more relevant to those found in flue gases from coal fired power stations [7].

Experimental Approach

We have investigated the interaction of the four previously studied alternative fuels (methanol, ethanol, M85, and E85, see Task 9) with NO in the presence of oxygen. The major aim was to identify and quantify the changes in the hydrocarbon, oxygenate species and examine the possible formation of nitrogen-containing products. The reaction products observed are compared to our previous results obtained without the addition of NO and with the recent engine tests of these fuels reported by SwRI [10] and the California Air Resources Board [11,12].

All experiments were conducted using the thermal decomposition analytical system (TDAS). The results of SwRI engine tests of these fuels indicated that the average NO_x concentrations, as measured under stoichiometric, federal test procedure (bag 3) engine dynamometer conditions, ranged from 240 ppm with methanol fuel to 280 ppm with ethanol fuel. The initial NO concentrations examined in our experiments were in a comparable range, i.e. 150 and 300 ppm. The TDAS was used in the same configuration as used for the recently completed thermal degradation studies of methanol, ethanol, M85, and E85. Experiments were conducted under fuel-lean ($\phi = 0.8$), stoichiometric ($\phi = 1.0$), and fuel-rich ($\phi = 1.1$) conditions. The fuel concentration varied slightly (300±75 ppmv), depending on the fuel-air-ratio. Experiments were conducted at temperatures of 500°C, 650°C and 800°C for a mean, gas-phase residence time of 0.8 s. The absolute pressure for all experiments was ~1.4 atm.

All reactants (fuel, O_2, N_2, NO) were admitted into the system in the gas-phase. A nitric oxide standard was obtained from Air Products and Chemicals, Inc. This standard (20.8% NO in helium) contained small amounts (<1%) of NO_2. Reactants were prepared in 2 liter Pyrex® sample bulbs. The reactants were isolated from ultraviolet radiation to ensure that no photolytic conversion occurred prior to thermal testing. A syringe pump was used to provide steady-state sample injection. High purity (99.99+%), moisture free helium was the diluent and reactor carrier gas.

The analytical procedures were identical to those described in Task 9. Temperature programmed capillary column gas chromatography was used for product separation. A porous layer OTC was used for separation of light hydrocarbons, oxygenates, and nitrogenated hydrocarbons. A quadrupole mass selective detector (MSD) was used for product detection. Surrogate organic analytical standards were used to confirm MSD identification of stable reaction byproducts. Semi-quantitation was obtained from least squares analysis of six point calibration curves.[2] Quantitative transport of NO throughout the reactor system was verified using off-line tedlar bag sampling and a chemiluminescent NO_x analyzer. Table 8.1 summarizes the GC-MS conditions for the experiments.

[2] The semi-quantitative data are not presented in this report. This data will be included in a subsequent report.

Table 8.1. GC-MS Conditions

GC Column:	GS-Q, 30 m x 0.32 mm i.d. PLOT column
GC Temperature Program:	-60°C to 230°C @ 10°C/min (GS-Q)
GC-MS Transfer Line Temperature:	250°C
Carrier Gas:	Helium
MS Ionization Mode	Electron Impact
MS Electron Energy:	70 eV
MS Electron Multiplier Setting:	2000 units
Mass Range Scanned:	10-200 amu

Experimental Results

We have examined the effect of NO addition in the range (150 and 300 ppmv) on the oxidation of methanol, M85, ethanol, and E85 at temperatures of 500, 650, and 800°C. A set of chromatograms that typify the effects observed are presented in the case of ethanol oxidation at 650°C in Figures 8.1a-8.1c.

Two general effects were observed for all four fuels. The addition of NO increased the conversion of each fuel to partial oxidation products. The primary effect was the increased yields of oxygenate species, e.g., formaldehyde from methanol and M85 and formaldehyde, acetaldehyde and dimethyl ether from ethanol and E85. A second effect observed was the increased yields of a wide range of reaction products. For example, for ethanol, addition of NO increased yields of pyrolysis-type products such as ethene, ethane, and acetylene (at higher temperatures). Increased yields of oxygenates were also observed with NO addition. Observed products included formaldehyde and dimethyl ether. These oxygenates were not observed in the oxidation of ethanol in the absence of NO addition. Ethyl formate and N-(hydroxymethyl)-2-propenamide were also observed that may be related to the presence of NO. The formation of N-(hydroxymethyl)-2-propenamide is speculative and will be subject to further analysis. At long retention times, it was evident that additional polar species had formed that could not be analyzed using conventional GC-MS analysis. Identification of these trace level products requires class separation (for polar compounds) and preconcentration coupled with sophisticated MDGC-MS analysis. This was beyond the scope of this task.

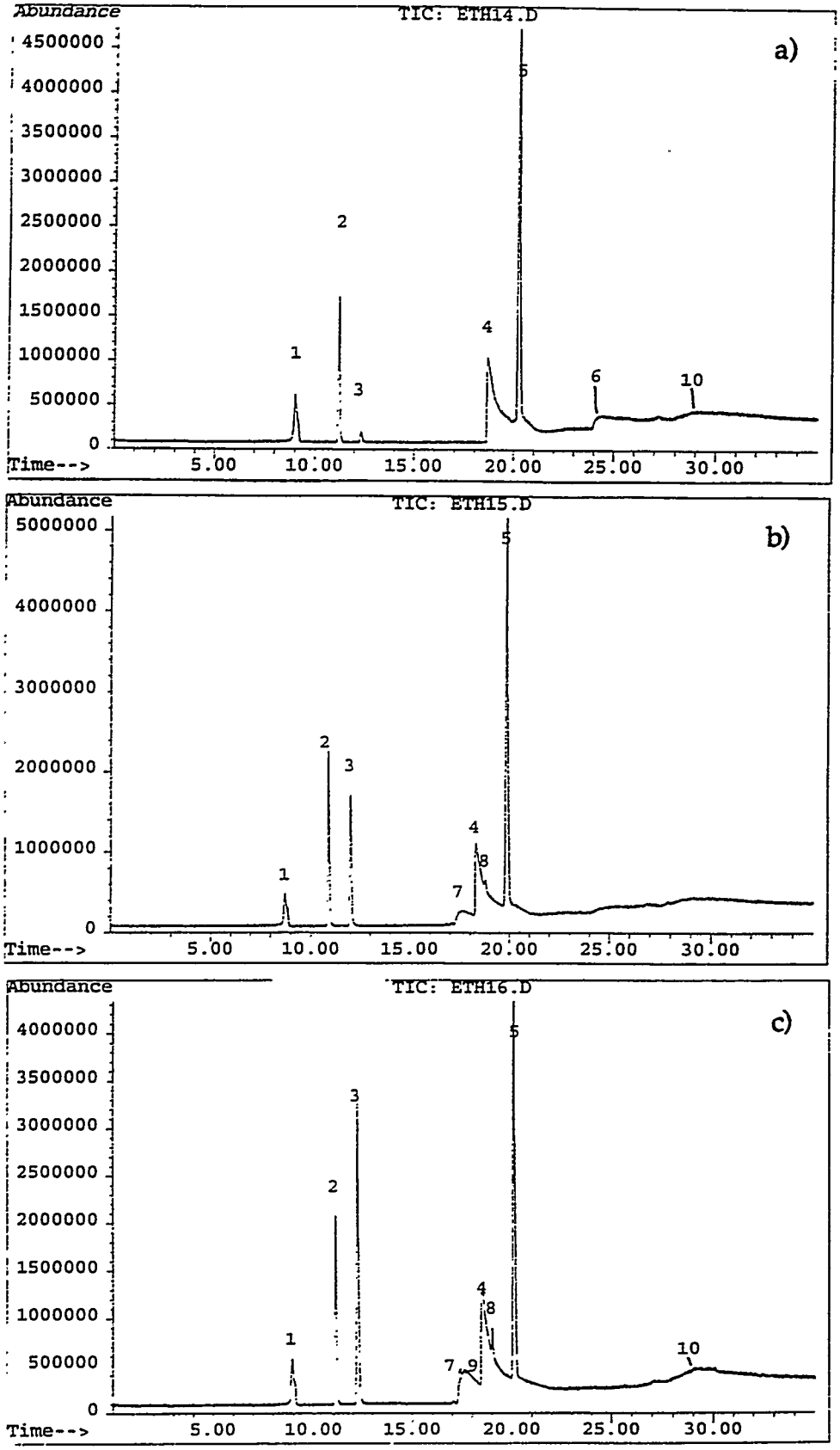

Figure 8.1 Total ion chromatograms from the NO perturbed oxidation of ethanol. T_r = 650°C. ϕ = 1.0. t_r = 0.8 s. (a) $[CH_3CH_2OH]_0$ = 300 ppm. (b) $[CH_3CH_2OH]_0$ = 300 ppm, $[NO]_0$ = 150 ppm. (c) $[CH_3CH_2OH]_0$ = 300 ppm, $[NO]_0$ = 300 ppm. Legend: 1: CO_2, 2: C_2H_4, 3: C_2H_6, 4: H_2O, 5: CH_3CHO, 6: CH_3CH_2OH, 7: CH_2O, 8: CH_3OCH_3, 9: N-(hydroxymethyl)-2-propenamide, 10: ethyl formate.

Tables 8.2-8.5 present observed reaction products for each fuel at a temperature of 650°C for different NO/fuel ratios. The number of x's in each column is indicative of quantitative increases or decreases in product yields with increasing NO loading.

Table 8.2
Organic Products from the Oxidation of Methanol at 650°C for Different NO/Fuel Ratios

	NO/Fuel Ratio[1]		
Compound	0	1/3	2/3
Formaldehyde	x	xx	xx
Methanol[2]	xxx	xx	x

[1] Unless noted, products were observed for all three fuel/air stoichiometries tested.
[2] Initial fuel component.

At 650°C, no additional reaction products were observed from NO perturbed methanol oxidation. The effect of NO addition involved enhanced conversion to formaldehyde. At 800°C, trace yields of ethene and ethane were observed. Under these higher temperature conditions, the addition of NO appeared to inhibit methanol conversion and result in formation of larger yields of these C_2 intermediates including acetylene. Hydrogen cyanide was also observed with NO addition at these elevated temperatures. These trends were independent of fuel/air stoichiometry.

Table 8.3
Organic Products from the Oxidation of M85 at 650°C for Different NO/Fuel Ratios

	NO/Fuel Ratio[1]		
Compound	0	1/3	2/3
Ethene	x	xx	xx
Ethane	x	xx	xx
Propene	x	xx	xx
Formaldehyde	x	xx	xx
Acetaldehyde[2]	x	xx	xx
Methanol[3]	xxx	xx	x
Ethanol[2,3]	xxx	xx	x
Benzene[3]	x	xx	xx
Toluene[3]	x	xx	xx
Ethylbenzene[3]	x	xx	xx
Xylene(s)[3]	x	xx	xx

[1] Unless noted, products were observed for all three fuel/air stoichiometries tested.
[2] Organic product observed under stoichiometric and fuel-rich conditions only.
[3] Initial fuel components as identified by GC-MS analysis.

A more dramatic effect was observed from NO perturbed M85 oxidation at 650°C. As observed for the neat methanol fuel, methanol conversion to formaldehyde increased with NO addition. However, a more complex effect was also evident. This involved increased yields of intermediate products ethene, ethane and propene. Benzene, toluene, ethylbenzene and xylene (fuel components) also exhibited slight increases in yields with NO addition. These trends were independent of fuel/air stoichiometry. Ethanol and acetaldehyde were also observed as reaction products under stoichiometric and fuel-rich conditions.

Table 8.4
Organic Products from the Oxidation of Ethanol at 650°C for Different NO/Fuel Ratios

	NO/Fuel Ratio[1]		
Compound	0	1/3	2/3
Ethene	x	xx	xxx
Ethane	x	xx	xxx
N-(hydroxymethyl)-2-propenamide		x	x
Formaldehyde		x	xx
Dimethyl ether		x	xx
Acetaldehyde	x	xx	xxx
Ethanol[2]	xxx	xx	x

[1] Unless noted, products were observed for all three fuel/air stoichiometries tested.

[2] Initial fuel component.

A rather dramatic effect was also observed from NO perturbed ethanol oxidation at 650°C. At this temperature, ethanol was nearly completely oxidized with acetaldehyde the primary product. Increased yields of the intermediate products ethene and ethane were also noted. Dimethyl ether, N-(hydroxymethyl)-2-propenamide, and formaldehyde were also observed as reaction products upon NO addition. These trends were independent of fuel/air stoichiometry.

Some additional experiments were also conducted at 500°C and 800°C. At 500°C, the effect of NO addition on ethanol oxidation was generally similar to the 650°C results. A notable exception was the formation of nitromethane with NO addition. The yields of nitromethane increased with increasing NO loading. Nitromethane was not observed in experiments conducted at 650°C and 800°C. At 800°C, the effect of NO addition on ethanol oxidation was somewhat different. The reaction products from ethanol oxidation were ethene, ethane, acetylene, propene and acetaldehyde. Addition of NO reduced the yields of ethene, ethane and acetaldehyde yet increased the yields of acetylene. The trace yields of propene did not appear to change significantly. In a surprising result, formaldehyde was observed as a reaction product with NO addition, even at these elevated temperatures. These trends were independent of fuel/air stoichiometry. In contrast to methanol, hydrogen cyanide was not observed for NO perturbed ethanol oxidation at these elevated temperatures.

Table 8.5
Organic Products from the Oxidation of E85 at 650°C for Different NO/Fuel Ratios

	NO/Fuel Ratio[1]		
Compound	0	1/3	2/3
Ethene	x	xx	xxx
Ethane	x	xx	xxx
Propene	x	xx	xxx
Formaldehyde		x	xx
Dimethyl ether		x	xx
Acetaldehyde	x	xx	xxx
Isobutylene[2]		x	xx
1,3-Butadiene		x	xx
Ethanol[2]	xxx	xx	x
Benzene[2]	x	xx	xxx
3-Methylhexane[2]	x	x	xx
n-Octane[2]	x	x	x
Toluene[2]	x	xx	xxx
Ethylbenzene[2]	x	x	xx
Xylene (3 isomers)[2]	x	x	xx

[1] Unless noted, products were observed for all three fuel/air stoichiometries tested.

[2] Initial fuel components as identified by GC-MS analysis.

The effect observed from NO perturbed E85 oxidation at 650°C was analogous to the M85 results. Ethanol conversion to acetaldehyde increased with NO addition. However, a more complex effect was also evident. This involved increased yields of intermediate products ethene, ethene, propene and formaldehyde and increased yields of initial fuel components including isobutylene, 3-methylhexane, octane, benzene, toluene, ethylbenzene and xylene. Dimethyl ether and 1,3-butadiene were also observed as reaction products with NO addition.

Similar results were obtained from NO perturbed E85 oxidation at 800°C. Ethanol conversion to acetaldehyde increased with increasing NO loading. Yields of a large number of secondary reaction products increased with increasing NO loading. These products included ethane, acetylene, propene, formaldehyde, 1,2-propadiene, dimethylether, isobutylene, 1,3-butadiene, 3-penten-1-yne, benzene, toluene, ethylbenzene, xylene and styrene. Ethene yields maximized at lower NO loadings.

Discussion

These results suggest that NO addition perturbs the oxidation chemistry in complex ways, acting perhaps as a catalyst with some fuel components and as an inhibitor with other fuel components. The manifestation of these effects may be controlled by temperature and NO concentration with fuel structure of lesser importance.

Previous researchers [1-5] have discussed mechanisms for the conversion of low concentrations of NO to NO_2 promoted by hydrocarbons. At low temperatures and high NO concentrations, it is generally agreed that the conversion is a result of reactions of the general type:

$$NO + RO_2 \Longrightarrow NO_2 + RO \qquad (R7.2)$$

where R = H, CH_3, C_2H_5, ..., C_nH_{2n+1}.

and that the addition of NO significantly perturbs the steady state concentration of the reactive OH radical. It is generally accepted that this class of reactions is also responsible for the conversion of NO to NO_2 in the free atmosphere, where subsequent photolysis of NO_2 results in ozone production and photochemical smog formation.

The effect of NO on the oxidation of 1-pentene at temperatures of 327-527°C has recently been reported [13]. Prabhu et al report that addition of small concentrations of NO (0-500 ppm) significantly altered 1-pentene oxidation as a result of competition between its promoting effect through reaction with HO_2 radicals (R7.3) and its retarding effect through reaction with OH radicals (R7.4):

$$NO + HO_2 \text{ -----> } NO_2 + OH \qquad \text{(R7.3)}$$

$$NO + OH + M \text{ -----> } HONO + M. \qquad \text{(R7.4)}$$

This effect is a function of the underlying fuel oxidation chemistry which generates HO_2 and OH radicals and the concentration of the NO added.

Molecular oxygen and hydroperoxy radicals are believed to the be key initiating species for the low-temperature conversion of methanol and ethanol to formaldehyde and acetaldehyde, respectively. As a result, our experiments appear to be consistent with the observations of Prabhu et al [13]. The reaction of NO with HO_2 to produce OH (R7.3) is thus proposed to explain the enhancement of reactivity in the presence of small amounts of NO. Chain termination, i.e., the reaction of NO with OH to produce nitrous acid (R7.4) is proposed to explain the inhibitory effect in the presence of larger quantities of NO. It is tempting to try to relate the inhibitory effect at elevated temperatures with the formation of pyrolysis-type products, e.g., ethene, ethane, propene, benzene, toluene, and xylene. However, detailed modeling of this system is necessary to further evaluate these effects.

An interesting result from Prabhu et al's experiments [13] was a NO_x deficit under certain experimental conditions. Preliminary analysis of the FTIR spectra and gas chromatograms obtained in their experiments indicated that reactions of NO_2 with alkyl radicals to form nitroalkanes contributes to the NO_x deficit:

$$R + NO_2 \text{ ------> } RNO_2. \qquad \text{(R7.5)}$$

We have also observed evidence for this reaction in the NO perturbed oxidation of ethanol at 500°C.

Comparison with Vehicle Tests

The available data [10-12] from engine tests of alternative fuels affords an opportunity to compare laboratory flow reactor and automotive emission results. In Tables 8.6-8.9, we qualitatively compare engine test results with our flow reactor tests conducted in the presence and absence of NO for methanol, M85, ethanol, and E85, respectively.

Table 8.6
Methanol Flow Reactor - Vehicle Comparison

Compounds observed in SwRI Vehicle Tests	UDRI Flow Reactor (w/o NO)	UDRI Flow Reactor (w/NO)
Methanol	x	x
Formaldehyde	x	x
Ethene	x	x
Ethane	x	x
Acetylene	x	x
Acetaldehyde	-	-
1,3-Butadiene	-	-
Benzene[1]	-	-
Toluene[1]	-	-

[1] Initial fuel components.

Prior to the NO experiments, the major difference between vehicle and flow reactor experiments of methanol oxidation was the detection of acetaldehyde, 1,3-butadiene, benzene, and toluene in the engine tests. Methanol oxidation in the presence of NO did not result in the formation of these compounds. This suggests that other mechanisms of formation of these compounds, e.g., crankcase oil leakage into the engine cylinder, are present in the engine tests. Evaporative canister purging is another possible source of these products, i.e., gasoline components stored in cannisters were purged during methanol fuel tests.

Table 8.7
M85 Flow Reactor - Vehicle Comparison

Compounds observed in CARB Vehicle Tests	UDRI Flow Reactor	UDRI Flow Reactor (w/NO)
Methanol	x	x
Formaldehyde	x	x
Ethene	x	x
Ethane	x	x
Propane	-	-
Acetaldehyde	-	x
Propene	-	x
n-Butane[1]	-	-
Methylbutane[1]	x	-
n-Pentane[1]	-	-
1,2,4-Trimethylbenzene	-	-
Ethylbenzene[1]		x
Toluene[1]	x	x
Xylene(s)[1]	x	x

[1] Initial fuel components.

The major difference between vehicle and flow reactor experiments of M85 oxidation was the detection of propane, acetaldehyde, propene, n-butane, methylbutane, n-pentane, ethylbenzene and trimethylbenzene in the engine tests. M85 oxidation in the presence of NO did result in the formation of acetaldehyde and propene, thus improving the comparison slightly. Compounds that have not been observed in the flow reactor experiments are dominated by straight-chain, alkane

fuel components. The relatively moderate thermal stability of these compounds under nominal oxidation conditions infers that a thermal quenching mechanism may be playing a role in their formation in the engine tests.

Table 8.8
Ethanol Flow Reactor - Vehicle Comparison

Compounds observed in SwRI Vehicle Tests	UDRI Flow Reactor (w/o NO)	UDRI Flow Reactor (w/NO)
Ethanol	x	x
Formaldehyde	-	x
Ethene	x	x
Ethane	x	x
Acetylene	x	x
Acetaldehyde	x	x
Acetic Acid	x	-
Propene	-	x
1,3-Butadiene	-	-
Benzene[1]	-	-

[1] Initial fuel components.

The major difference between vehicle and flow reactor experiments of ethanol oxidation was the detection of formaldehyde, propene, 1,3-butadiene and benzene in the engine tests. Ethanol oxidation in the presence of NO did result in the formation of formaldehyde and propene. 1,3-Butadiene and benzene are higher molecular weight components. The formation of these compounds is enhanced under oxygen-deficient conditions. This infers that localized, fuel-rich zones of residual fuel may be playing a role in their formation in the engine tests. Evaporative canister purging is another possible source of these products, i.e., gasoline components stored in cannisters were purged during ethanol fuel tests.

Table 8.9
E85 Flow Reactor - Vehicle Comparison

Compounds observed in CARB Vehicle Tests	UDRI Flow Reactor (w/o NO)	UDRI Flow Reactor (w/NO)
Ethanol	x	x
Formaldehyde	-	x
Acetylene	x	x
Ethene	x	x
Ethane	x	x
Propane	-	-
Acetaldehyde	x	x
Propene	x	x
Isobutylene[1]	-	x
n-Butane[1]	x	-
2,2,4-Trimethylpentane[1]	-	-
Trimethylbenzene	-	-
3-Ethyltoluene	-	-
Toluene[1]	x	x
Xylene (3 isomers)[1]	x	x

[1] Initial fuel components.

The major difference between vehicle and flow reactor experiments of E85 oxidation was the detection of formaldehyde, propane, isobutylene, 2,2,4-trimethylpentane, trimethylbenzene and 3-ethyltoluene in the engine tests. E85 oxidation in the presence of NO did result in the formation of formaldehyde and isobutylene, thus improving the comparison. Compounds that have not been observed in the flow reactor experiments include both straight-chain, alkane fuel components and higher molecular weight aromatic compounds. The moderate to high thermal stability of these compounds under nominal oxidation conditions infers that both thermal quenching and localized poor mixing failure modes may be playing a role in their formation in the engine tests.

Summary

Experiments of the NO perturbed oxidation of methanol, M85, ethanol, and E85 have been completed for temperatures ranging from 500-800°C. At mild temperatures, NO addition results in enhanced fuel conversion. At elevated temperatures, an inhibitory effect was observed through increased yields of both partial oxidation and pyrolysis-type reaction products. Changes in the concentrations of initator radicals, i.e., HO_2 and OH radicals, are proposed to account for the experimental observations. Comparison of flow reactor product distributions with vehicle results generally indicated improved comparisons when NO was added to the fuel. However, differences in product distributions remain and are likely due to different failure mode mechanisms that have not been fully addressed in the previous flow reactor tests.

References

1. Hori, M. 1986. 21st Symp. (Int.) on Combust., The Combustion Institute, p. 1181.
2. Bromly, J. H., Barnes, F. J. and Little, L. H. 1988. J. Inst. Energy, 61, 89.
3. Bromly, J. H., Barnes, F. J., Mandyczewski, R., Edwards, T. J., and Haynes, B. S. 1992. 24th Symp. (Int.) on Combust., The Combustion Institute, p. 899.
4. Hori, M., Matsunaga, N., Malte, P. C. and Marinov, N. M. 1992. 24th Symp. (Int.) on Combust., The Combustion Institute, p. 909.
5. Bromly, J. H. 1991. The Formation of Nitrogen Oxides in Gas Combustion, Ph.D. Thesis, Murdoch University.
6. Johnson, G. M. and Smith, M. Y. 1978. Combust. Sci. Technol., 19, 67.
7. Nelson, P. F. and Haynes, B. S. 1994. 25th Symp. (Int.) on Combust., p. 1003, The Combustion Institute.
8. Mallard, W. G., Westley, F., Frizzell, D. H. Herron, J. T. and Hampson, R.F. 1993. NIST Chemical Kientics Data base Varsion 5.0, NIST, Gaithersburg, MD.
9. Atakan, B., Kocis, D., Wolfrum, J. and Nelson, P.F. 1992. 24th Symp. (Int.) on Combust., The Combustion Institute, p. 691.
10. Whitney, K. 1995. "Determination of Alternative Fuels Combustion Products", NREL/TP-425-7528, Golden, CO: National Renewable Energy Laboratory.
11. California Air Resources Board. 1991. "Proposed Reactivity Adjustment Factors for Transitional Low-Emissions Vehicles-Staff Report and Technical Support Document," September 27.
12. California Air Resources Board. 1994. "Preliminary Reactivity Adjustment Factors," Mobile Sources Division, El Monte, CA.
13. Prabhu, S.K., Bhat, R.K., Miller, D.L., and Cernansky, N.P. 1996. Combustion Flame, 104, 377.

Task 9. Formation of Pollutants from the Secondary Components of Alternative Fuel Formulations

Introduction

Research on hydrocarbon emissions from the combustion of conventional gasoline reveal that the secondary components (e.g., alkenes, arenes) can have a significant contribution to the measured pollutant emissions. In this study, we augment our thermal decomposition data set by studying fully formulated fuels, the primary components, and secondary (or even tertiary) components that would be predicted to have a possibly significant effect on pollutant emissions. In this way we can determine the true source of pollutant formation and devise strategies for improving formulations to minimize emissions.

This task thus involves a comparative study of the stable reaction byproducts produced from the thermal degradation of pure methanol and ethanol versus methanol and ethanol containing 15% gasoline, i.e., M85 and E85. The major aim was to identify and quantify the organic emissions and determine the influence of significant changes in fuel composition on the observed emissions. Specifically, this task presents the results of the controlled, high-temperature thermal degradation of methanol, ethanol, M85, and E85. We have quantified thermal degradation products from the fuel-lean, stoichiometric, and fuel-rich oxidation of all four fuels. The cumulative, quantitative emissions data are presented as nonmethane organic gases (NMOG) and total oxygenates. Specific reactivity (SR), a measure of grams of the ozone formation by photochemical reaction per gram of nonmethane organic exhaust gases, has been calculated for each fuel using standard maximum incremental reactivity (MIR) factors developed by the California Air Resources Board. MIR factors used in SR calculations were taken from the listing of Tsuchiida et al [1].

Experiments at gas temperatures in the vicinity of 600°C to 800°C may be of particular significance because they encompass the temperature range of post-combustion conversion of residual fuel in the exhaust port and runner of a spark-ignited engine [2,3]. Hydrocarbon evolution in the exhaust port and runner leading to the catalytic converter is of considerable importance because a significant fraction (~33%) of the cylinder-out hydrocarbons are oxidized in the port/runner [4]. Furthermore, before catalyst light-off, the catalyst is cold and ineffective so that oxidation in the exhaust port/runner is the major hydrocarbon removal process outside of the engine cylinder [3].

A comparison of organic products for each fuel is presented. NMOG distributions for methanol, ethanol, M85 and E85 are compared with vehicle results conducted by SwRI [5] and the California Air Resources Board [6,7]. The formation of previously unidentified organic products is discussed.

Experimental Approach

Quantitative experiments were performed using a 1.1 cm i.d. fused silica flow reactor coupled to a GC/MS analytical system. A block diagram of this system is shown in Figure 9.1. The design of this system has been discussed in detail previously [8]. This paper focuses instead on a brief description of the operational and analytical features pertinent to these experiments.

Research grade methanol and ethanol samples were purchased from Aldrich Chemical Co. M85 and E85 were supplied by SwRI. All samples were used as received.

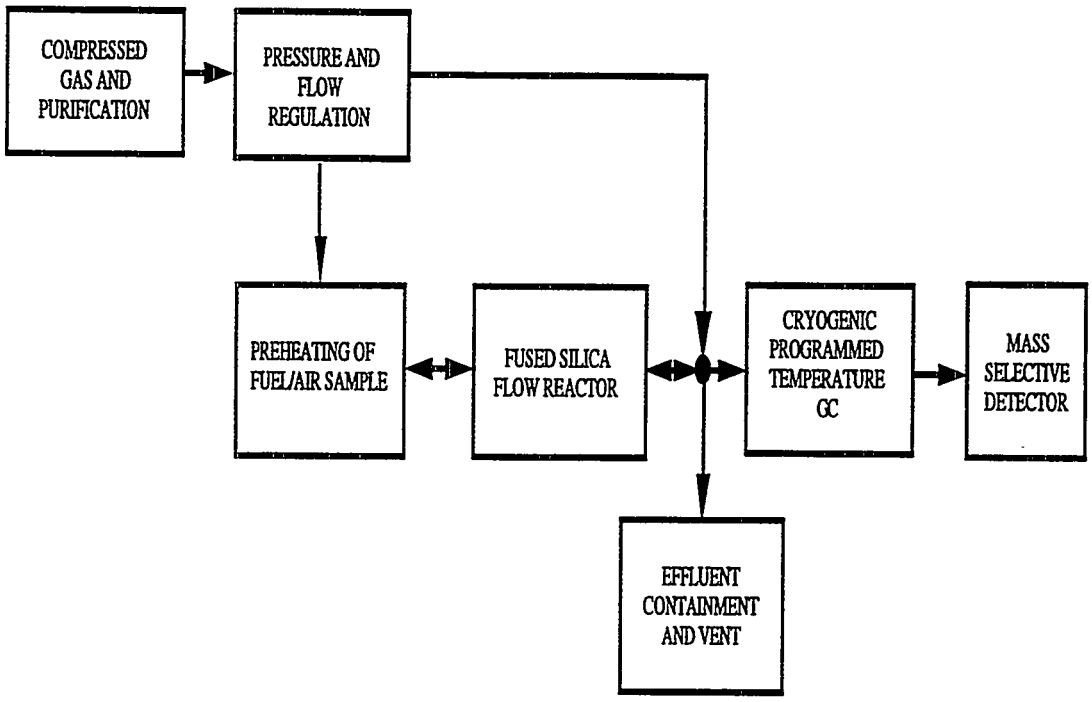

Figure 9.1. Block diagram of the modified Thermal Decomposition Analytical System.

Experiments were conducted for three different fuel/air equivalence ratios (ϕ) ranging from fuel-lean to fuel-rich (fuel/air equivalence ratio is defined as the actual fuel/air molar ratio divided by the stoichiometric fuel/air molar ratio). The fuel/air equivalence ratio was controlled by *a priori* mixing of liquid fuel aliquots with moisture-free air in previously cleaned and dried glass sample vessels of known volume (415 cm^3). Table 1 summarizes the initial fuel/air equivalence ratio and reactor concentrations (at 650°C) examined in this work. Relatively low initial fuel concentrations resulted from large carrier gas (He) flow rates. The reactor mean, gas-phase residence time ($t_r = 0.85$ s) and pressure (p ~1.4 atm) were constant for all experiments. Experiments were conducted at four different exposure temperatures: 500°C, 650°C, 800°C and 950°C.

Following metered gas-phase sample injection and high-temperature exposure, the thermal degradation products were swept by helium carrier gas through an ice-cooled, glass frit held at ~0°C and then to the head of a GC column held at -60°C [9]. The porous frit effectively trapped water vapor during the data acquisition portion of the experiments. The reduced quantities of water present in the GC column permitted baseline GC separation and quantification of water-insoluble organic products.[3] During the analytical portion of the experiments, the ice-water was removed and the frit was allowed to equilibrate to ambient temperatures. Water insoluble organic products (and a fraction of the water) were then purged from the frit using high purity helium carrier gas. Trial and error procedures were conducted to determine the optimum duration (5 minutes) of carrier gas purging. The possibility of residual organic condensation products associated with the frit was further checked by conducting high-velocity carrier gas purging for a duration of 60 minutes followed by GC analysis. No residual organic products were observed from these tests.

[3] Formaldehyde was the only oxygenated product observed that could not be resolved using this procedure, due to its high affinity for water. Formaldehyde was quantified using extracted ion analysis (m/e = 29).

Table 9.1. Initial Fuel/Air Equivalence Ratios and Reactor Concentrations

Fuel	ϕ	Input Reactor Concentration, ppm(v/v)
Methanol	0.8	265
	1.0	325
	1.1	355
Ethanol	0.8	210
	1.0	260
	1.1	280
M85	0.8	250
	1.0	305
	1.1	335
E85	0.8	180
	1.0	225
	1.1	245

The reactor effluent, after passing through the high-temperature reactor and glass frit, was swept to the gas chromatograph using high-purity helium carrier gas. Before reaching the inlet of the GC column, a 820:1 split between the reactor and the GC directed only a minute portion of the effluent to the column. The majority of the effluent was passed through an activated charcoal trap before venting to the atmosphere. Capillary column gas chromatography was used for product separation. The effluent resulting from a single reactor exposure (unreacted parent material and reaction products) was directed to a 30-m, megabore 0.32-mm i.d., GS-Q porous layer open tubular column (J & W Scientific, Inc.). Individual reaction products were separated by programming the GC oven from -60°C to 230°C @ 10°C/min. Following GC separation, product detection was accomplished using a mass selective detector in the full-scan mode. The following analytical standards were used to provide semi-quantitative analysis of thermal reaction products: acetaldehyde, ethanol, n-hexane, and o-xylene. Calibration curves were linear for all four standards ($r^2 > 0.99$). The calibration curve for ethanol was used to quantify both methanol and ethanol. The calibration curve for acetaldehyde was used to quantify carbonyl-containing compounds. The calibration curves for n-hexane and o-xylene were used to quantify aliphatic and aromatic hydrocarbons, respectively.

The repeatability of a given experiment and the resulting effluent yields was ±20%. Uncertainties in semi-quantitative product yields based on uncertainties in sample preparation, flow calibrations, reactor temperature, and residence time for major and minor products were ±10% and ±25%, respectively. The focus of these studies was quantitation of organic reaction products. No attempt was made to quantitate carbon monoxide or molecular oxygen, nor was any attempt made to quantify the formation of NO_x.

Results

To establish the range of product formation from the four alternative fuels, experiments were initially conducted at temperatures of 500°C, 600°C, 700°C, and 800°C. For all fuels, very limited decomposition was observed at 500°C. For M85 and E85, benzene, toluene, xylene (3 isomers), and ethylbenzene were the largest, identified hydrocarbon components of the unreacted gasoline component of the fuel at 500°C. Experiments at 600°C and 700°C indicated significant product formation for all fuels. Identifiable products are given in Tables 9.2 and 9.3 (*vide infra*).

A summary of identifiable organic products from the oxidation of methanol/M85 and ethanol/E85 is given in Tables 9.2 and 9.3, respectively. With the exception of E85, organic products were only observed for temperatures between 600°C and 700°C. Experiments at 800°C and 950°C

indicated complete conversion of the fuel to thermodynamic end-products carbon dioxide and water vapor. Observed products from methanol were nearly identical to our previous studies [9] and were dominated by formaldehyde and unburned methanol. Small amounts of ethane were also observed for all three stoichiometries tested. Observed products from ethanol were also very similar to our previous studies [9]. The major products were acetaldehyde and unburned ethanol. Minor products included C_2-hydrocarbons, formaldehyde, and acetic acid. Two previously unidentified species, 2,6-dimethylbenzaldehyde and ethylbenzaldehyde, were also observed from ethanol oxidation. These species were only observed under stoichiometric conditions.

Table 9.2
Organic Products from the Oxidation of Methanol and M85

	Fuel[1]	
Compound	Methanol	M85
Formaldehyde	x	x
Methanol[3]	x	x
Ethene	x	x
Ethane	x	x[2]
Dimethoxymethane	x	x
2-Ethoxy-1-propanol		x
2-Methylpropene[3]		x[2]
Methyl propyl ether		x
2-Methylpropene		x
2-Methylbutane[3]		x
2-Methylpentane[3]		x
2,3-Dimethylpentane[3]		x
Heptane[3]		x
Benzene[3]		x
Toluene[3]		x
Xylene[3] (3 isomers)		x

[1] Unless noted, products were observed for all three fuel/air stoichiometries tested.
[2] Organic product observed under fuel-rich conditions only.
[3] Initial fuel component.

As expected, a much larger number of products were identified from the oxidation of M85 and E85. For M85, these products included species associated with methanol that have been previously identified, the most stable of the aliphatic and aromatic hydrocarbon species associated with gasoline, and three species that have not been previously identified. These "new" species were dimethoxymethane, 2-ethoxy-1-propanol, and methyl propyl ether. The atmospheric reactivity of these species is apparently unknown and may or may not be appreciable. These three species were observed under all three stoichiometries tested. For E85, observed products included species associated with ethanol that have been previously identified and the most stable of the aliphatic and aromatic hydrocarbon species associated with gasoline. A larger number of stable aliphatic hydrocarbons were observed from E85 than M85. The composition of this effluent consisted of several unsaturated C_5 and C_6 hydrocarbons. 2-Pentene exhibited the highest yield of these species. It is noteworthy that the three previously unidentified oxygenated species observed from M85 oxidation were not observed from E85 oxidation.

E85 was the only fuel which produced several, measurable organic products at 950°C. Unfortunately, these species were difficult to identify with the NIST standard reference mass spectral library. One species that was tentatively identified (mass spectral match quality of ~50%)

was propionic acid. Propionic acid was observed only under fuel-lean conditions. Several additional peaks were observed under fuel-lean conditions that could not be identified.

Table 9.3
Organic Products from the Oxidation of Ethanol and E85

	Fuel[1]	
Compound	Ethanol	E85
Formaldehyde	x	x
Ethene	x	x
Ethane	x	x
Ethanol[3]	x	x
Acetylene	x	x
Acetaldehyde	x	x
Acetic Acid	x[2]	
Propene	x	x
Propionic acid		x[4]
n-Butane[3]		x
2-Methylbutane[3]		x
2-Pentene[3]		x
2-Methylpentane[3]		x
2,3-Dimethylpentane[3]		x
2-Methyl-1-pentene[3]		x
1-Hexene[3]		x[5]
Heptane[3]		x
Benzene[3]		x
Toluene[3]		x
Xylene[3] (3 isomers)		x
Nonane[3]		x[6]
2,6-Dimethylbenzaldehyde	x[7]	
Ethylbenzaldehyde	x[7]	

[1] Unless noted, products were observed for all three fuel/air stoichiometries tested.
[2] Organic product observed under fuel-lean and stoichiometric conditions only.
[3] Initial fuel component.
[4] Organic product observed under fuel-lean conditions only.
[5] Organic product observed under stoichiometric and fuel-rich conditions only.
[6] Organic product observed under fuel-rich conditions only.
[7] Organic product observed under stoichiometric conditions only.

The cumulative, quantitative emissions data for the four alternative fuels, expressed as NMOG (non-methane organic gases per gram of injected fuel), are summarized in Figure 9.2 as a function of fuel/air equivalence ratio for an exposure temperature of 650°C.

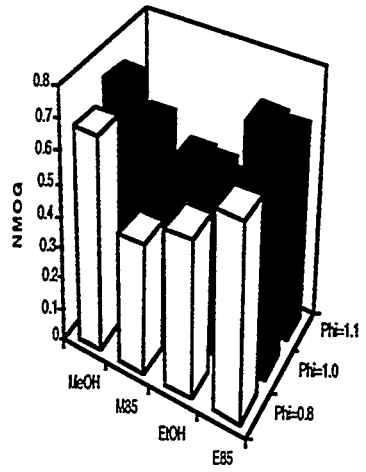

Figure 9.2. NMOG yields normalized to the mass of fuel injected as a function of fuel type and fuel/air equivalence ratio. T_r = 650°C. t_r = 0.85 s.

A relatively small variation in NMOG among the four fuels was observed. M85 generally had the lowest NMOG yields, followed by ethanol. NMOG yields were also relatively insensitive to fuel/air equivalence ratio.

Figure 9.3 presents data for total oxygenates (normalized to the mass of fuel injected) observed from the four alternative fuels at a temperature of 650°C.

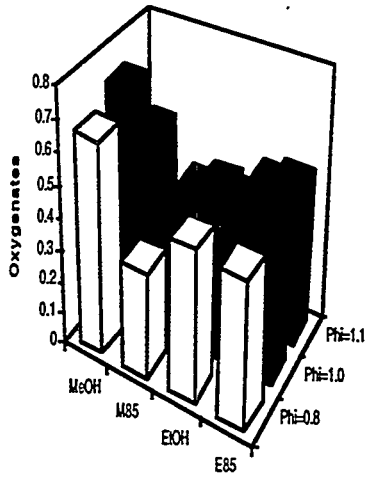

Figure 9.3. Oxygenate yields normalized to the mass of fuel injected as a function of fuel type and fuel/air equivalence ratio. T_r = 650°C. t_r = 0.85 s.

Comparison of the data in Figures 9.2 and 9.3 indicates that most of the observed NMOG was oxygenate compounds. This percentage varied from 75% (for E85 for $\phi = 0.8$) to greater than 98% (for methanol for $\phi = 0.8$). M85 had the lowest oxygenate yields for all three fuel/air equivalence ratios tested.

Discussion

In order to assess the atmospheric impact of alternative fuel combustion product emissions, the specific reactivity (SR) of the exhaust gas was calculated for each fuel based on quantification of NMOG emissions. The SR is defined as the grams of ozone produced in the atmosphere per gram of NMOG emissions from a fuel. SR is a function of MIR, which defines the atmospheric reactivity of each exhaust species:

$$SR = \sum_i (M_i \times MIR_i / \sum M_i) \qquad \text{(Eq 9.1)}$$

where: M_i = mass of NMOG species i in the exhaust, and MIR_i = maximum incremental reactivity of species i in the exhaust. Methane was not included in the calculation of SR because of its negligibly small MIR (0.01). The MIR factors, calculated by the California Air Resources Board, were taken from a recently listing of Tsuchida et al [1] and have not been updated since 1991.

Figure 9.4 presents SRs for all four fuels as a function of equivalence ratio for an exposure temperature of 650°C.

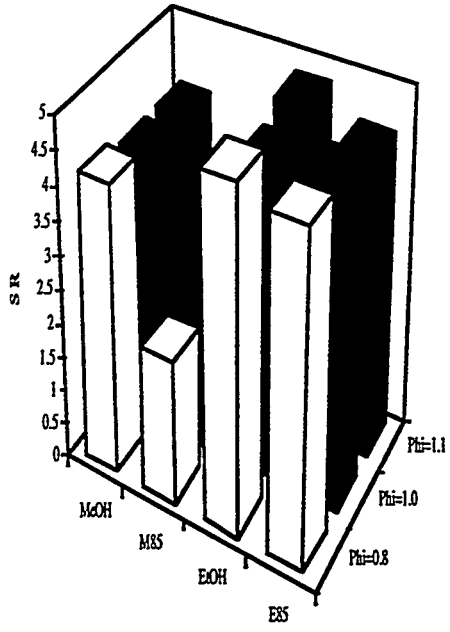

Figure 9.4. Specific reactivity calculated using maximum incremental reactivity factors as a function of fuel type and equivalence ratio. T_r = 650°C. t_r = 0.85 s.

M85 had the lowest SR for all three stoichiometries tested. The specific reactivities of the other three fuels were roughly equal (~4-5) and did not vary with stoichiometry. The specific reactivity of M85 was lowest under fuel-rich conditions. It is noteworthy that while the SR of ethanol and E85 were not significantly different (~4.4-4.7), the SR of M85 was substantially less than that of methanol. Examination of speciated product yields indicated that reduced yields of formaldehyde from the oxidation of M85 was responsible for the observed decrease. It should be noted that the SR reported in this study at 650°C are somewhat higher than typically reported with vehicle tests (≤ 3). The measurements at 650°C may represent a near worst-case condition for several of these fuels and may not be directly related to the results of a cumulative vehicle emission test.

The specific reactivity of methanol, ethanol, and M85 at 950°C was essentially zero due to the lack of formation of any organic products. A specific reactivity at 950°C for the E85 fuel was not calculable based on the lack of available MIR values for the tentative species identifications.

The recently completed engine tests of alternative fuels affords an opportunity to compare laboratory flow reactor and automotive emission results reported by Southwest Research Institute for methanol and ethanol [5] and the California Air Resources Board for M85 and E85 [6,7]. It is instructive to begin with a simple, qualitative comparison.

The quantified emission products of the "neat" alcohol fuels were remarkably consistent. For methanol, organic products in common with both sets of data were unburned fuel, formaldehyde, ethane, and ethene. For ethanol, organic products in common with both sets of data were unburned fuel, formaldehyde, acetaldehyde, ethane, ethene, acetylene, and propene (trace). The most significant differences in the "neat" fuel comparisons were the lack of detection of acetylene, benzene, acetaldehyde, and acrolein from the flow reactor studies of methanol degradation, and the lack of detection of 2,2-dimethylbutane, benzene, and acrolein from the flow reactor studies of ethanol degradation. Many of these products, e.g., acetylene and benzene, have been observed in pyrolytic flow reactor studies of these fuels, indicating the likelihood that localized fuel-rich stoichiometries play a significant role in vehicle emissions.

A comparison of the organic products for M85 and E85 also yielded generally consistent results. For M85, organic products in common with both engine tests and flow reactor experiments included methanol, formaldehyde, ethene, ethane, methylbutane, toluene, and the three xylene isomers. For E85, common products included ethanol, formaldehyde, acetaldehyde, ethane, ethene, acetylene, propene, butane, toluene, and the three xylene isomers. The most significant differences in the M85 fuel comparisons was the formation of three additional oxygenated species in the flow reactor experiments. These products were identified as dimethoxymethane, 2-ethoxy-1-propanol, and methyl propyl ether. The flow reactor experiments also produced several initial fuel components (methyl-substituted alkanes) that were not generally detected in the vehicle tests. The most significant differences in the E85 fuels comparisons was the formation of three highly reactive, unsaturated alkenes in the flow reactor experiments. These products were identified as 2-pentene, 2-methyl-1-pentene, and 1-hexene. These unsaturated compounds are present in some gasoline formulations and are typical exhaust components of gasoline vehicles. Vehicle tests also produced several likely fuel components (methyl- and ethyl-substituted aromatic species) that were not observed in the flow reactor experiments.

We have previously reported quantitative comparisons of organic emission products for methanol, ethanol, natural gas, and LP gas from stoichiometric engine tests [5] and flow reactor experiments conducted at different exposure temperatures [10]. The best quantitative emission comparisons for the "neat" alcohol fuels was obtained at relatively low temperatures, that is, 400°C and 600°C for ethanol and methanol, respectively. Generally consistent emission comparisons for natural gas and LP gas were obtained at a higher temperature (750°C). Tables 9.4 and 9.5 present a quantitative comparison of NMOG emissions from the previously described flow reactor experiments at a temperature of 650°C and the vehicle tests for M85 and E85, respectively [6,7]. The flow reactor data were normalized to the total mass fraction of NMOG species quantified. The engine test data were provided as mass percent of NMOG species and used without correction.

Table 9.4
M85 Flow Reactor (650°C) - Vehicle Comparison
(Product yields in mass %)

Compound	Vehicle	Flow Reactor
Methanol	80.0	55.0
Formaldehyde	6.1	24.7
Dimethoxymethane	bdl[1]	0.9
Ethene	1.0	1.5
Ethane	0.2	bdl
Propane	0.05	bdl
Acetaldehyde	0.2	bdl
Propene	0.5	bdl
2-Ethoxypropanol	bdl	2.3
n-Butane	1.1	bdl
Methylbutane	0.7	1.5
n-Pentane	0.4	bdl
2-Methylpentane	bdl	1.5
2,3-Dimethylpentane	bdl	1.5
Benzene	bdl	3.1
1,2,4-Trimethylbenzene	0.3	bdl
n-Heptane	bdl	1.4
Toluene	1.5	3.3
Xylene (3 isomers)	0.9	3.3

[1] Below detection limits.

As evident in Tables 9.4 and 9.5, the quantified emissions comparison were not as favorable as previously found for methanol and ethanol. This was not necessarily unexpected because of the increased complexity of these fuels compared with "neat" methanol and ethanol. The largest disagreement was observed for the unburned fuel and its primary partial oxidation product, e.g., methanol and formaldehyde from M85 and ethanol and acetaldehyde from E85. Although overall agreement of organic emissions was not achieved, several species did exhibit similar yields (±5%, excluding undetectable species) among the two different tests. For M85, these products included ethene, methylbutane, toluene, and the xylene isomers. For E85, these products included formaldehyde, ethene, ethane, acetylene, propene, n-butane, and the xylene isomers.

The disparity in the comparisons presented here may be related to several factors. The emissions reported in vehicle tests may be controlled by various failure modes outlined at the introduction of this report (cf. Table 1.1) that are not addressed in these experiments, e.g., oil layer oxidation/pyrolysis, reactions on surfaces, different sampling and analysis procedures, fuel memory from evaporative emission canisters, etc. Furthermore, the vehicle data are a composite average of many engine tests with different vehicles. The FTP results presented in the California Air Resources Board report may also be dominated by cold-start (bag 1) emissions, or unburned fuel emissions. A more appropriate comparison for the reactor tests would be the bag 2 results of the stabilized portion of the vehicle test procedure. This segment may have less unburned fuel emissions components and more partially burned emission components.

Table 9.5
E85 Flow Reactor (650°C) - Vehicle Comparison
(Product yields in mass %)

Compound	Vehicle	Flow Reactor
Ethanol	72.8	10.6
Formaldehyde	1.9	trace
Acetylene	1.8	1.2
Ethene	4.8	1.4
Ethane	1.8	1.2
Propane	0.2	bdl[1]
Acetaldehyde	7.8	66.4
Propene	0.5	1.2
2-Methylpropene	0.2	bdl
n-Butane	1.4	1.2
2-Methylbutane	bdl	1.3
2-Pentene	bdl	1.2
2-Methylpentane	bdl	1.3
1-Hexene	bdl	1.2
2-Methyl-1-pentene	bdl	1.2
2,3-Dimethylpentane	bdl	1.2
Benzene	bdl	1.4
Trimethylbenzene	0.5	bdl
n-Heptane	bdl	1.2
Toluene	bdl	2.8
3-Ethyltoluene	0.1	bdl
Xylene (3 isomers)	0.8	2.7

[1] Below detection limits.

Summary

The thermal degradation of methanol, M85, ethanol, and E85 has been examined in flow reactor experiments at temperatures of 500°C, 650°C, 800°C, and 950°C for a gas-phase residence time of 0.85 s. All four fuels were observed to be completely degraded at 950°C, with little degradation observed at 500°C. NMOG emissions from methanol, ethanol, M85, and E85 were observed to be more sensitive to exposure temperature than fuel/air equivalence ratio. NMOG emissions were largely below detection limits at 950°C. At 650°C, a large majority of NMOG emissions consisted of oxygenated species. Specific reactivities of M85 were observed to be substantially lower than for the other fuels. This was due to the reduced quantities of formaldehyde observed in the M85 experiments. Several previously unidentified species were observed in these experiments which may impact atmospheric reactivity assessments of these fuels. These species included dimethoxymethane, 2-ethoxy-1-propanol, methyl propyl ether, propionic acid, 2,6-dimethyl-benzaldehyde and ethylbenzaldehyde. A qualitative comparison of organic speciation for these fuels with recent vehicle tests [5-7] produced remarkably similar results. A quantitative comparison of major NMOG species showed considerable disparity. The disagreement between the two sets of data was hypothesized to be related to several factors including the various failure modes outlined at the beginning of this report (cf. Table 1.1) that were not addressed in this task.

References

1. Tsuchida, H. Ishihara, K., Iwakiri, Y. and Matsumoto, M. 1993. SAE Technical Paper Series No. 932718, Warrendale, PA.
2. Drobot, K., Cheng, W. K., Trinker, F. H., Kaiser, W., Siegl, W. O., Cotton, D. F., and Underwood, J. 1994. Combust. Flame, 99, 422.
3. Cheng, W. K., Hamrin, D., Heywood, J. B., Hochgreb, S., Min, K. and Norris, M. 1993. SAE Technical Paper Series No. 932708, Warrendale, PA.
4. Caton, J. A., Heywood, J. B., and Mendillo, J. V. 1984. Combust. Sci. Technol., 37, 153.
5. Whitney, K. 1995. NREL/TP-425-7528, Golden, CO: National Renewable Energy Laboratory.
6. California Air Resources Board. 1991. "Proposed Reactivity Adjustment Factors for Transitional Low-Emissions Vehicles - Staff Report and Technical Support Document, Sacramento, CA, September 27.
7. California Air Resources Board. 1994. "Preliminary Reactivity Adjustment Factors," Mobile Sources Division, El Monte, CA.
8. Rubey, W. A. and Carnes, R. A. 1985. Rev. Sci. Instrum., 56, 1795.
9. Shanbhag, S., Taylor, P.H. and Dellinger, B. 1995. "The Origin and Fate of Organic Pollutants from the Combustion of Alternative Fuels," proceedings of the Windsor Workshop on Alternative Fuels, Toronto, Ontario, Canada.
10. Shanbhag, S., Taylor, P.H. and Dellinger, B. 1996. "Organic Pollutants from the Combustion of Alternative Fuels," proceedings of the 11th International Symposium on Alcohol Fuels, Sun City, South Africa.

Task 10. Low Temperature Surface Catalyzed and Gas-Phase Pollutant Formation

Introduction

The main objective of this project was to investigate the pollutant formation reactions in the engine exhaust system. The reactions occurring in the exhaust system can contribute significantly to overall engine emissions. Results of recent studies have shown that many organic compounds, e.g., dioxins, furans, and nitro-PAHs, are formed in the post combustion-zone of many devices.[1] The post combustion zone, sometimes referred to as the "cool zone", can be subdivided into a gas quench zone and a surface catalysis zone. The automobile exhaust zone is very similar to the combustor cool zone, being characterized by the presence of particles, relatively low temperatures and longer residence times. Nitro-PAHs and other high molecular weight carcinogens have been observed in diesel exhaust.[2] There is a high probability that some of these high molecular weight compounds are formed in exhaust systems of vehicles burning alternative fuels. This premise can be extended to suggest that pollutants formed upstream of exhaust system may undergo further reactions to form other pollutants.

In this study we addressed pollutant formation in the automobile exhaust zone by examining surface reactions of alternative fuels that have survived the combustion chamber and are contained in the engine exhaust gas. Specifically, this task presents the results of controlled, thermal degradation of methanol and ethanol over a Pd/Rh catalyst. Our choice of catalyst was based on literature review of current catalyst technology to control automotive emissions from conventional and alternative fuels. From this review, we concluded that the Pd/Rh three way catalyst is the most promising catalyst to reduce emissions from vehicles using alternative fuels.[3] We have also conducted experiments with and without nitric oxide, NO in order to understand the effect of NO on pollutant formation at cold start temperatures. It is well-known that trace quantities of NO can effect hydrocarbon oxidation (see Task 8 and [4,5]). However, to our knowledge, there have been no studies conducted on the effect of NO at cold start temperatures in the presence of catalyst. We believe this is the first experimental study to investigate NO effect on hydrocarbon combustion under these conditions.

Experimental Approach

This task was conducted on our System for Thermal Diagnostic Studies (STDS). The STDS is a continuous, in-line flow reactor system which can be used to simulate the reaction conditions in the automobile exhaust zone. The design of STDS has been discussed in detail elsewhere.[6] This report gives a brief description of the operational and analytical features pertinent to this task. The STDS consists of four integrated units: 1) a control console for precise adjustment of temperature, pressure, residence time, and carrier gas flow; 2) a thermal reactor compartment (TRC) that is housed within an HP 5890 gas chromatograph (GC) to allow precise temperature control of sample lines into and out of the reactor; 3) a gas chromatographic chamber (HP 5890 GC) for separation of products; and 4) a mass selective detector (HP 5970B MSD) for product identification and quantitation. A unique advantage of STDS reactor assembly is its versatility as it can house different types of reactors to emulate different reaction conditions. A schematic diagram of the STDS is shown in Figure 10.1.

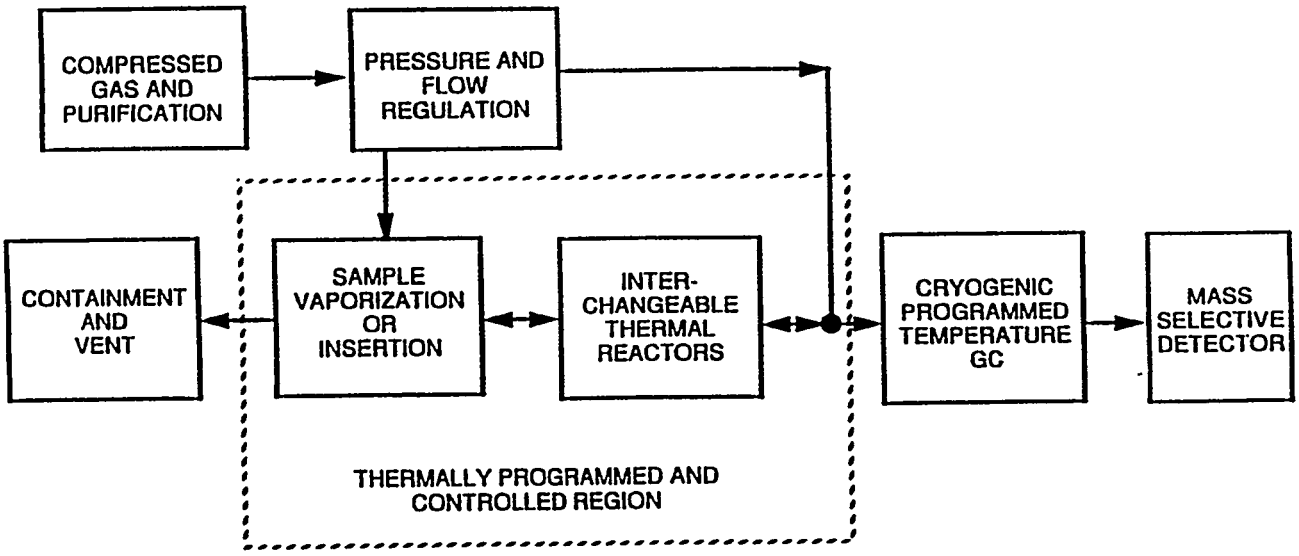

Figure 10.1 Schematic Diagram of System for Thermal Diagnostic Studies.

For this task, the thermal reactor chamber of the STDS housed a 0.3 cm i.d. stainless steel tubular packed bed reactor to investigate gas-surface reactions. The tubular reactor was packed with a Pd/Rh catalyst. The catalyst was prepared by mixing 10 wt% Rh with Pd and weighed 0.5 gm. Both Pd and Rh were coated on alumina particles of 60 mesh size. Experiments were conducted under stoichiometric (ϕ= 1.0) conditions. A fuel concentration of 1000 ppmv was maintained in all experiments to represent the unburnt fuel entering the automobile exhaust zone. Vapor-phase fuel along with stoichiometric air, prepared and premixed *a priori* in 415 cm^3 Pyrex® sample bulbs, were injected into the insertion chamber using a calibrated syringe pump. The diluent gas consisted of 9% CO_2 in helium to emulate the post-combustion effluent. Two different fuels were tested: methanol and ethanol. For the NO experiments, NO (500ppmv) was injected into the reactor along with fuel-air mix. Experiments were conducted at temperatures of 50°C, 100°C, 150°C, 200°C, 300°C, 400°C, and 500°C. Experiments were conducted at reactor residence times of 200 ms. The time and temperatures were chosen to emulate the conditions in an exhaust system under which surface reactions may occur.

The resulting gas-phase effluents from each series of experiments were analyzed using in-line GC-MS and GC-FID. Temperature programmed capillary column gas chromatography was used for product separation. We used a parallel two column approach to analyze reactor effluents. A porous layer open tubular column (PLOT) was used for fixed gas analysis and wall coated open tubular column (WCOT) for organic analysis. Detectors for these columns were an FID and an HP 5970B MSD, respectively. The WCOT was constructed by attaching BPX70 (20m length) and DB-1 (5 μ film thickness, 30 m length) columns in series. This combination gave us the capability to trap and analyze light products like formaldehyde (DB-1) and heavy products like nitro-PAHs (BPX70). The effluents were collected in the analytical GC chamber at -60°C (cooled by liquid nitrogen). After each run, the temperature of the analytical GC was programmed from -60°C (2 min. hold) to 240°C (10 min. hold) at a rate of 10°C/min. No attempt was made to quantify NO/NO_2 or the organic reaction products.

Results

Oxidation of both methanol and ethanol was effected by addition of NO. NO inhibited oxidation of both oxygenated fuels and produced different nitrogenated products for each set of experiments.

Methanol

Methanol oxidation over Pd/Rh resulted in formation of methyl formate, methyl carbonate and water at 50°C (cf. Figure 10.2). At 100°C, acetone and methyl acetate were formed along with the products seen at 50°C. Methyl formate was the dominant product and methanol was completely destroyed at both these temperatures. At higher temperatures, no organic products were observed.

When NO (500 ppm) was added to the reactor gas, it inhibited the oxidation of methanol as methanol was observed at both 50 and 100°C (cf. Figure 10.3). Addition of NO also produced several nitrogen-containing products, i.e., nitroethane, 2-nitrobenzaldehyde, and substituted 1H-imidazole along with the other products observed in the previous set of methanol experiments. One similarity between these two sets of experiments was that no products were observed at temperatures $\geq$ 150°C.

Ethanol

Ethanol oxidation at 50°C over Pd/Rh resulted in formation of acetaldehyde, methanol, acetone, isopropyl alcohol, ethyl formate, and methyl, ethyl, isopropyl, and vinyl acetate along with unconverted ethanol. Isopropyl alcohol was the major product (cf. Figure 10.4). At 100°C, the same products were observed with ethyl acetate being the dominant product. At 150°C, ethanol oxidation was nearly complete with the organic product yields maximized; acetic acid was the major product. At 200°C, ethanol and most of the products were oxidized; only small amounts of acetone, methyl and ethyl acetate were observed. At 300°C and higher, no organic products were observed.

As observed in the methanol experiments, addition of NO (500 ppm) also inhibited oxidation of ethanol at 50, 100, and 150°C (cf. Figure 10.5). Addition of NO produced ethyl nitrite at 50°C and acetonitrile and diacetylamine at 150°C. All other products were similar to the previous set of experiments without NO. No organic products were observed at temperatures $\geq$ 300°C.

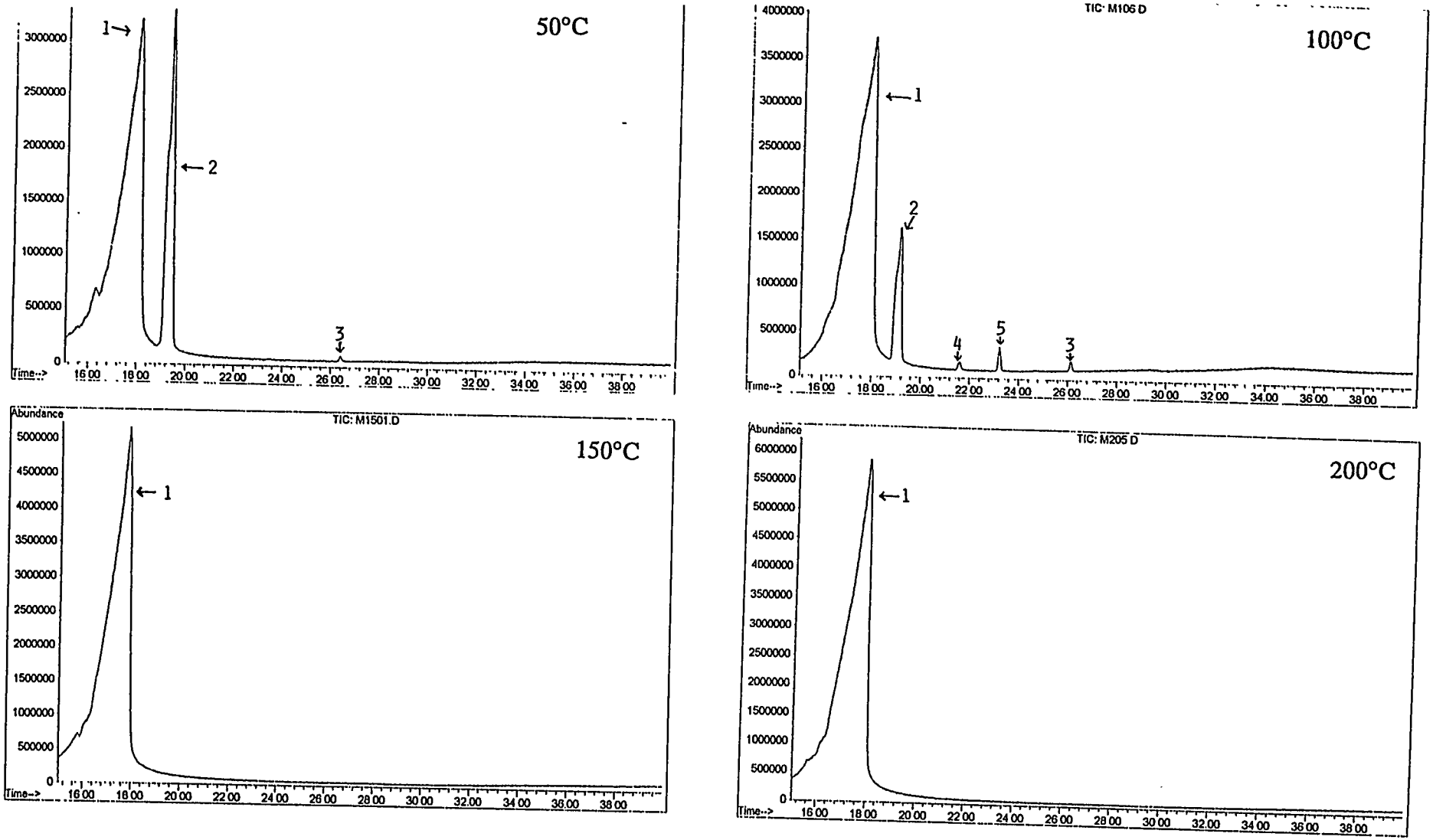

1- Water
2- Methyl Formate
3- Methyl Carbonate
4- Acetone
5- Methyl Acetate

Figure 10.2 Chromatograms of stoichiometric oxidation of methanol (1000 ppm) over Pd/Rh catalyst in reactor gas containing 9% CO_2 in helium for residence time of 200 ms, at 50°C, 100°C, 150°C, and 200°C.

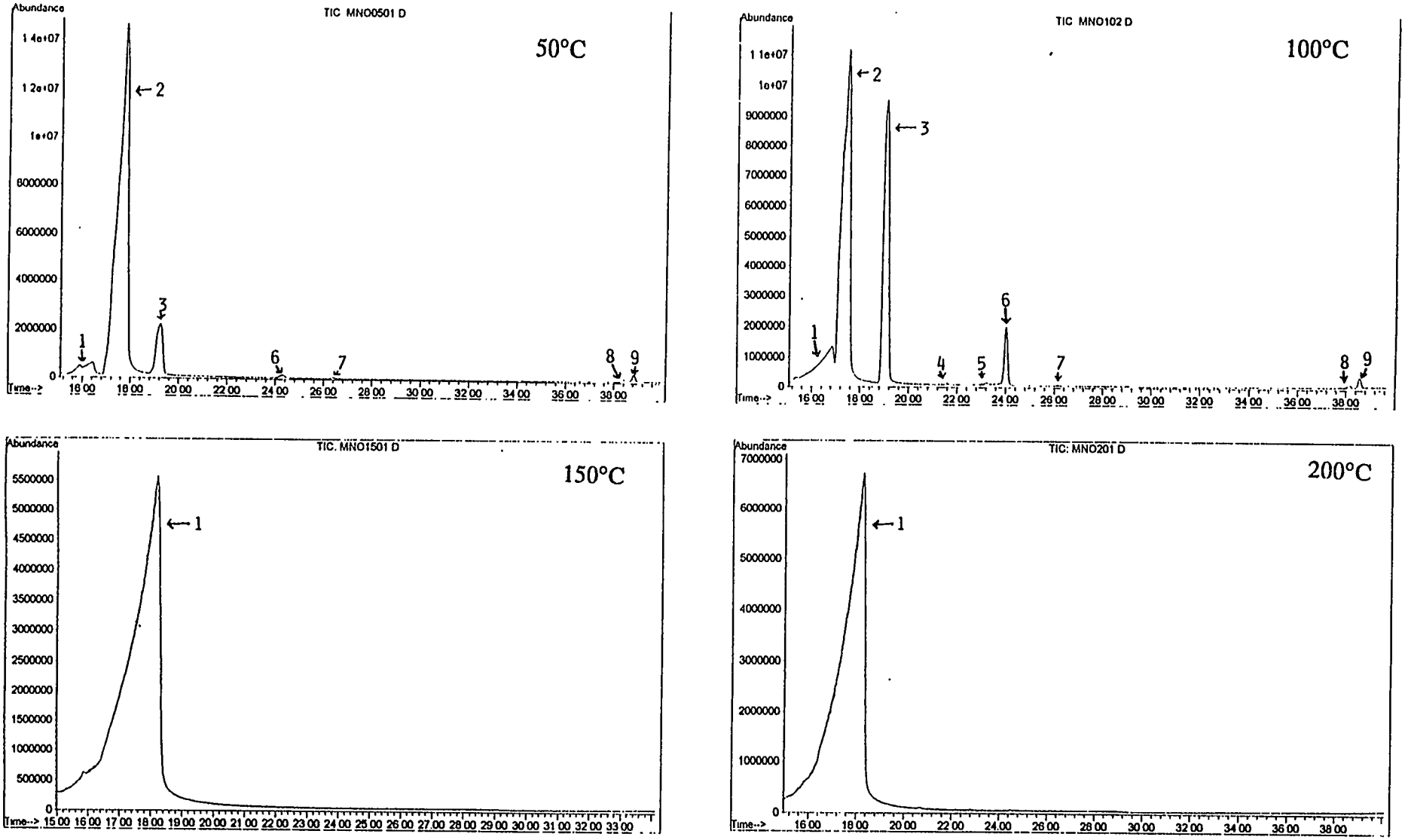

1- Water
2- Methanol
3- Methyl Formate
4- Acetone
5- Methyl Acetate
6- Nitro Ethane
7- Methyl Carbonate
8- 2-Nitrobenzaldehyde
9- Substituted 1-H Imidazole

Figure 10.3 Chromatograms of stoichiometric oxidation of methanol (1000 ppm) in presence of NO (500 ppm) over Pd/Rh catalyst in reactor gas containing 9% CO_2 in helium for residence time of 200 ms, at 50°C, 100°C, 150°C, and 200°C.

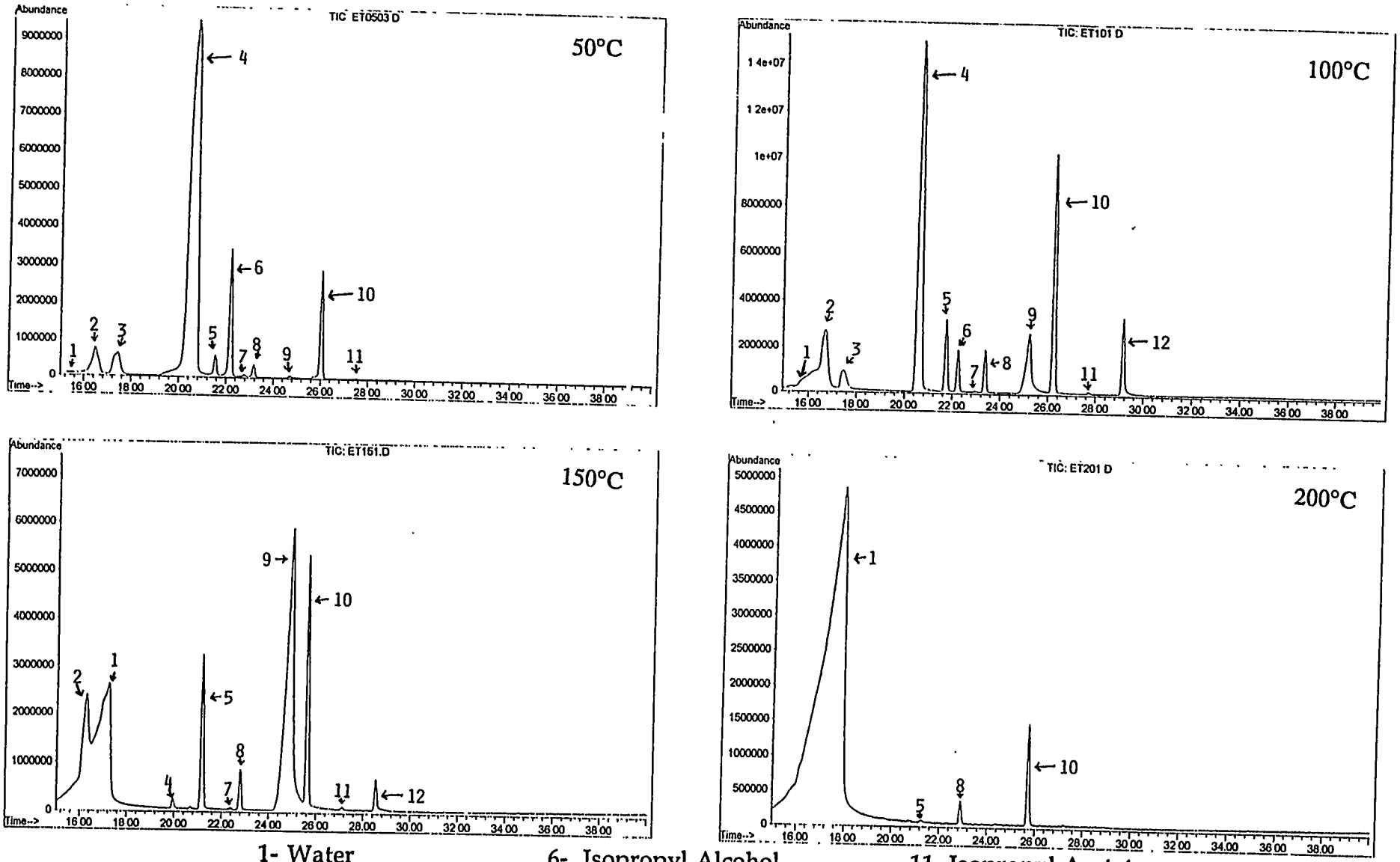

1- Water
2- Acetaldehyde
3- Methanol
4- Ethanol
5- Acetone
6- Isopropyl Alcohol
7- Ethyl Formate
8- Methyl Acetate
9- Acetic Acid
10- Ethyl Acetate
11- Isopropyl Acetate
12- Vinyl Acetate

Figure 10.4 Chromatograms of stoichiometric oxidation of ethanol (1000 ppm) over Pd/Rh catalyst in reactor gas containing 9% CO_2 in helium for residence time of 200 ms, at 50°C, 100°C, 150°C, and 200°C.

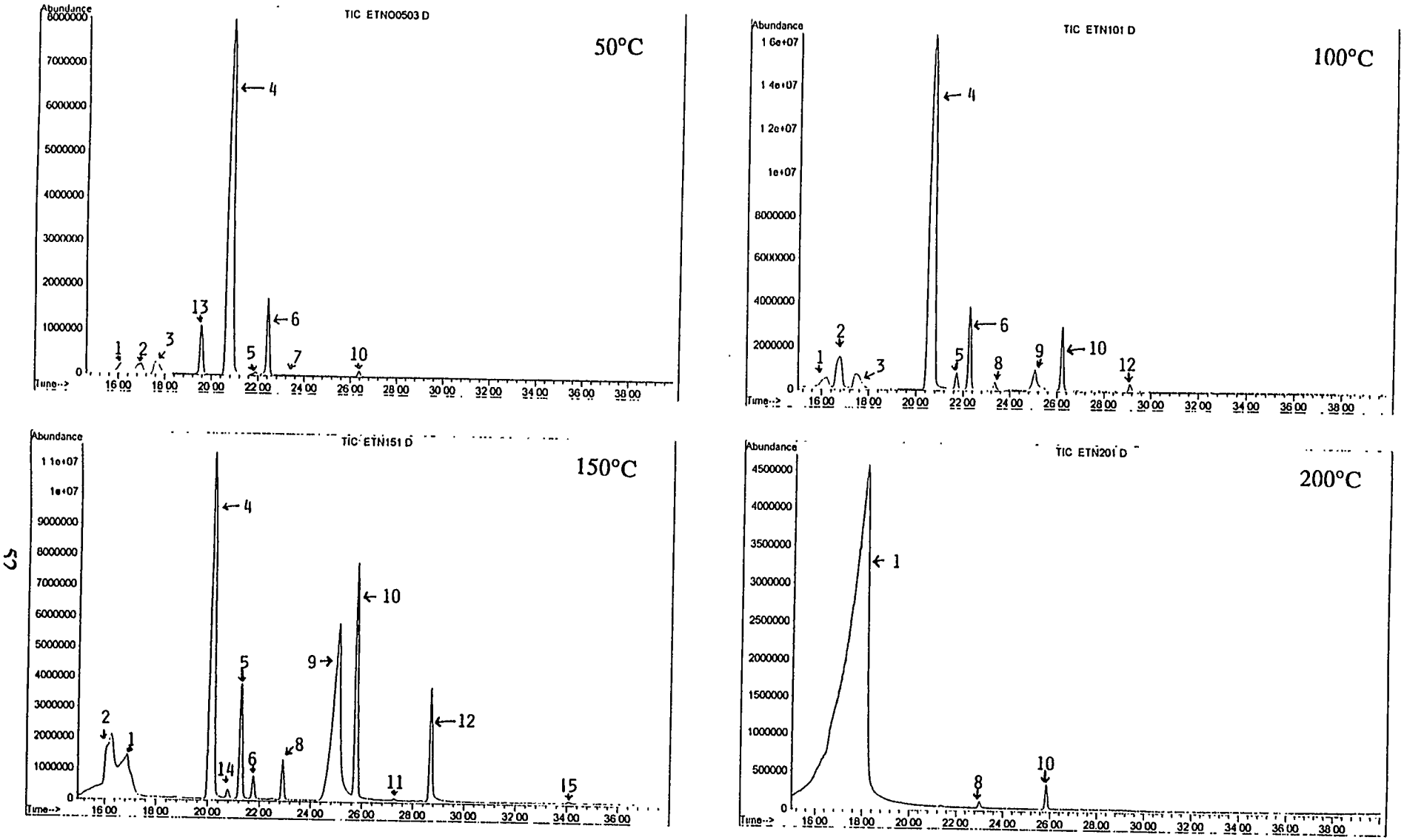

1- Water
2- Acetaldehyde
3- Methanol
4- Ethanol
5- Acetone
6- Isopropyl Alcohol
7- Ethyl Formate
8- Methyl Acetate
9- Acetic Acid
10- Ethyl Acetate
11- Isopropyl Acetate
12- Vinyl Acetate
13- Ethyl Nitrite
14- Acetonitile
15- Diacetyl amine

Figure 10.5 Chromatograms of stoichiometric oxidation of ethanol (1000 ppm) in presence of NO (500 ppm) over Pd/Rh catalyst in reactor gas containing 9% CO_2 in helium for residence time of 200 ms, at 50°C, 100°C, 150°C, and 200°C.

Discussion

This study of methanol and ethanol oxidation (with and without NO) over a Pd/Rh catalyst has shown that most of the pollutants are formed at temperature ≤ 200°C. We also observed that addition of NO inhibits the oxidation of methanol and ethanol over a Pd/Rh catalyst and it also forms nitrogen-containing products. This result differs from that observed in our higher temperature gas-phase studies described in Task 8. In the higher temperature studies, the effect of NO was temperature dependent. At intermediate temperatures (≤650°C), a promoting effect was observed that was hypothesized to be related to conversion of less reactive HO_2 radicals to more reactive OH radicals. At higher temperatures (≥800°C), an inhibitory effect was observed. Elucidation of the mechanistic aspects of NO inhibition in the gas-surface studies described here requires characterization of the catalyst surface in addition to comprehensive, time-dependent product analysis studies.

Nearly all of the products that were observed in this study have not been observed in engine emissions tests. We hypothesize that a probable reason for this is the differences in analytical sophistication between the two sets of analyses. We are using a very sophisticated in-line GC-column arrangement which enables us to observe fragile oxygenated and nitrogenated products. This kind of analytical system is not typically employed in engine emission tests. [7,8]

We also observed that at temperatures ≥ 200°C, the oxidation of ethanol and methanol was complete. However, pollutant emissions are observed at temperatures ≥ 200°C in engine emission tests.[8] This disagreement between these two sets of data could be related to the following:

(1) Our reactor system controls residence time and temperature very precisely, whereas the engine exhaust system has wide residence time and temperature distributions. One way to resolve this question will be to vary residence time and observe its effect on pollutant formation.

(2) In our experiments, we used the very efficient Pd/Rh catalyst. Engine exhaust systems used during engine emission tests may have been using different and aged catalysts. This can be resolved by examining different catalysts.

(3) The results from our study has shown that NO has a profound effect on ethanol and methanol oxidation. In this study we used only one concentration of NO (500 ppm), however, NO concentrations engine exhaust system could vary over a wide range. To resolve this issue, experiments over a range of NO concentration must be examined.

Summary

Laboratory-scale experiments of the conversion of neat methanol and ethanol over a Pd/Pt catalyst have resulted in a number of partially oxidized reaction products that have not been reported in engine tests [7,8] or higher temperature, post-combustion, laboratory-scale, gas-phase oxidation studies.[9-11] These compounds have relatively low reactivities with OH radicals compared to the typically measured aldehyde byproducts. MIR values for these compounds are probably comparable to long-chain alkanes. As a result, their impact on tropospheric smog formation may be fairly minimal.

The health effect impacts of these compounds, on the other hand, may be a significant issue. Certain oxygen-containing compounds have been implicated as potential endocrine disrupter chemicals.[12] A detailed, multi-dimensional GC analysis of the effluent from these experiments would be a worthy experiment.

The results of this study have also raised questions about the effect of some key fundamental parameters, e.g. time and temperature distributions throughout the catalyst, on pollutant formation in engine exhaust systems. These questions can also be further addressed by an additional series of well designed, laboratory experiments.

References

1. Goldfarb, T. D. 1989. Chemosphere 18, 1051.
2. Schuetzle, D., and Perez, J.M. 1983. J. Air Poll. Cont. Assoc., 33, 751.
3. Engler, B.H., Lindner, D., Lox, E.S., Schaefer-Sindlinger, A., and Ostgathe, K. 1995. Stud. Surf. Sci. Catal., 96, 441.
4. Bromly, J.H., Barnes, F.J., Mandyczewski, R., Edwards, T.J., and Haynes, B. S. 1992. 24th Symp. (Int.) on Combust., The Combustion Institute, p. 899.
5. Nelson, P.F., and Haynes, B.S. 1992. 25th Symp. (Int.) on Combust., The Combustion Institute, p. 1003.
6. Rubey, W.A., and Grant, R.A. 1988. Rev. Sci. Instrum., 59, 265.
7. Whitney, K.A., "Determination of Alternative Fuels Combustion Products, 1995. NREL/TP-425-7528, Golden, CO: National Renewable Energy Laboratory.
8. Whitney, K.A., "Determination of Alternative Fuels Combustion Products, 1996. NREL/TP-425-xxxx, Golden, CO: National Renewable Energy Laboratory.
9. Taylor, P.H., Shanbhag, S., and Dellinger, B. 1994. in Progress in Emission Control Technologies (SP-1053), SAE Technical Paper Series #941904, p. 39, Warrendale, PA.
10. Shanbhag, S., Taylor, P.H., and Dellinger, B. 1996. "The Origin and Fate of Organic Pollutants from the Combustion of Alternative Fuels," presented at the 11th International Symposium on Alcohol Fuels, Sun City, South Africa.
11. Taylor, P.H., Cheng, L., and Dellinger, B. 1996. in Alternative Fuel: Composition, Performance, Engines, and Systems (SP-1181), SAE Technical Paper Series #961088, p. 269, Warrendale, PA.
12. Colborn, T., vom Saal, F.S., and Soto, A.M. 1993. Environ. Health Perspect. 101, 378.

REPORT DOCUMENTATION PAGE

Form Approved
OMB NO. 0704-0188

1. AGENCY USE ONLY (Leave blank)	2. REPORT DATE	3. REPORT TYPE AND DATES COVERED
	June 1997	Subcontract report

4. TITLE AND SUBTITLE

The Origin of Organic Pollutants from the Combustion of Alternative Fuels: Phase IV Report

5. FUNDING NUMBERS

(C) XAU-3-12228-02
(TA) FU703610

6. AUTHOR(S)

P.H. Taylor, B. Dellinger, S. Sidhu, W. Rubey, R. Striebich, L. Cheng

7. PERFORMING ORGANIZATION NAME(S) AND ADDRESS(ES)

University of Dayton Research Institute
300 College Park
Dayton, OH 45469-0132

8. PERFORMING ORGANIZATION REPORT NUMBER

DE97050816

9. SPONSORING/MONITORING AGENCY NAME(S) AND ADDRESS(ES)

National Renewable Energy Laboratory
1617 Cole Boulevard
Golden, CO 80401-3393

10. SPONSORING/MONITORING AGENCY REPORT NUMBER

NREL/SR-540-23145

11. SUPPLEMENTARY NOTES

12a. DISTRIBUTION/AVAILABILITY STATEMENT

National Technical Information Service
U.S. Department of Commerce
5285 Port Royal Road
Springfield, VA 22161

12b. DISTRIBUTION CODE

UC-1504

13. ABSTRACT *(Maximum 200 words)*

The research described in this report resulted from laboratory experiments of the conversion of neat methanol and ethanol over a Pd/Pt catalyst. These experiments resulted in a number of partially oxidized reaction products that have not been reported in engine tests, or in higher temperature, post-combustion, lab-scale, gas-phase oxidation studies. These compounds have relatively low reactivities, so their impact on tropospheric smog formation may be fairly minimal. However, the health effect impacts of these compounds may be a significant issue. Further study is needed on these compounds and their effect on human health.

14. SUBJECT TERMS

Alternative fuels, transportation fuels, air quality, health effects

15. NUMBER OF PAGES

54

16. PRICE CODE

17. SECURITY CLASSIFICATION OF REPORT	18. SECURITY CLASSIFICATION OF THIS PAGE	19. SECURITY CLASSIFICATION OF ABSTRACT	20. LIMITATION OF ABSTRACT